European Journal of Medicinal Chemistry 220 (2021) 113472

Contents lists available at ScienceDirect

European Journal of Medicinal Chemistry

journal homepage: http://www.elsevier.com/locate/ejmech

Synthesis of alkynylated 1,2,4-oxadiazole/1,2,3-1*H*-triazole glycoconjugates: Discovering new compounds for use in chemotherapy against lung carcinoma and *Mycobacterium tuberculosis*

Valentina Nascimento Melo de Oliveira [b], Cybele Flávia do Amaral Moura [a], Aline dos Santos Peixoto [c], Vanessa Pinheiro Gonçalves Ferreira [d, e], Héverton Mendes Araújo [d, e], Lilian Maria Lapa Montenegro Pimentel [c], Claudia do Ó Pessoa [d], Roberto Nicolete [d, e], Janaína Versiani dos Anjos [b], Prem Prakash Sharma [f], Brijesh Rathi [f], Lindomar José Pena [g], Patrick Rollin [h], Arnaud Tatibouët [h], Ronaldo Nascimento de Oliveira [a, *]

[a] *Department of Chemistry, Federal Rural University of Pernambuco, Dois Irmãos, 52171-900, Recife, Brazil*
[b] *Department of Fundamental Chemistry, Federal University of Pernambuco, 50.740-540, Recife, Brazil*
[c] *Department of Immunology, Aggeu Magalhães Institute, Oswaldo Cruz Foundation, Brazil*
[d] *Laboratorio de Oncologia Experimental, Nucleo de Pesquisa Em Desenvolvimento de Medicamentos (NPDM), Universidade Federal Do Ceara, Fortaleza, Brazil*
[e] *Oswaldo Cruz Foundation (Fiocruz), Eusebio, Brazil*
[f] *Laboratory for Translational Chemistry and Drug Discovery, Department of Chemistry, Hansraj College University Enclave, University of Delhi, Delhi, India*
[g] *Department of Virology, Oswaldo Cruz Foundation, Fiocruz, 50740-465, Recife, PE, Brazil*
[h] *Universite D'Orleans et CNRS, ICOA, UMR 7311, BP 6759, F-45067, Orleans, France*

ARTICLE INFO

Article history:
Received 21 January 2021
Received in revised form
8 April 2021
Accepted 9 April 2021
Available online 18 April 2021

Keywords:
Glycerosugar
1,2,3-Triazole
1,2,4-Oxadiazole
Antitubercular activity
Antiproliferative activity
MD simulations

ABSTRACT

A total of forty-three compounds were synthesized, including thirty-two new ones. Among those compounds, seventeen were selected and tested on human tumor cell lines: PC-3 (prostate adenocarcinoma), HCT-116 (colorectal tumor), NCIH-460 (lung carcinoma), SKMEL-103 (melanoma) and AGP-01 (gastric tumor). Alkynylated 1,2,4-oxadiazoles **2m**, **3g** and **3k** exhibited antiproliferative activities against NCIH-460 in culture. Alkynylated *N*-cyclohexyl-1,2,4-oxadiazoles **3a-m** and bis-heterocycle glucoglycero-1,2,3-triazole-*N*-cyclohexyl-1,2,4-oxadiazole derivatives **5a-k** and **6**–**11** were evaluated for their *in vitro* efficacy towards *Mycobacterium tuberculosis* (*Mtb*) H_{37}Ra and H_{37}Rv strains. In general, glycerosugars conjugated to 1,2,4-oxadiazole via a 1,2,3-triazole linkage (**5a**, **5e**, **5j**, **5k**, and **7**) showed *in vitro* inhibitory activity against *Mtb* (H_{37}Rv). The largest molecules bis-triazoles **10** and **11**, proved inactive against TB. Probably, the absence of the *N*-cyclohexyl group in compound **8** and 1,2,4-oxadiazole nucleus in compound **9** were responsible for its low activity. Glucoglycero-triazole-oxadiazole derivatives **5e** (10 μM) and **7** (23.9 μM) were the most promising antitubercular compounds, showing a better selective index than when tested against RAW 264.7 and HepG2 cells. Vero cell were used to investigate cytotoxicity of compounds **5a**, **5h**, **5j**, **5k**, and these compounds showed good cell viability. Further, *in silico* studies were performed for most active compounds (**5e** and **7**) with potential drug targets, DprE1 and InhA of Mtb to understand possible interactions aided with molecular dynamic simulation (100ns).

* Corresponding author.
E-mail address: ronaldo.noliveira@ufrpe.br (R. Nascimento de Oliveira).

https://doi.org/10.1016/j.ejmech.2021.113472
0223-5234/

1. Introduction

Since the 1990s, studies in glycobiology have increased considerably and aroused the interest of organic chemists for the development of new synthetic methodologies aiming at the conjugation between carbohydrates and compounds oaf biological interest. When such compounds come from non-natural sources, glycoconjugates are called neo-glycoconjugates [1–3]. This new approach could not only provide data for studying some cellular phenomena not yet fully elucidated, but also supply new bioactive substances [4].

According to the World Health Organization (WHO) "Tuberculosis (TB) is a major yet preventable global health problem, with an estimated 10 million people developing TB and 1.5 million people dying every year worldwide, making it the leading infectious disease cause of death worldwide" [5]. Although therapeutic schemes are available for the treatment of tuberculosis, the emergence of resistant strains due to resistance mechanisms has hampered healing process and increased death cases [6]. These findings show that the development of new anti-TB agents is imperative [7]. TB is an infectious disease affecting the lungs that causes death especially in developing countries [8].

Cancer is the second leading cause of death globally accountable for human casualties, 8.8 million in 2015 and 9.6 million in 2018 [9]. Lung carcinoma is the leading cause of death by cancer. It is an aggressive tumor with reduced survival rate, showing a high prevalence of bone metastasis [10]. Tuberculosis is one of the risk factors for cancer; numerous studies have been conducted in this thematic, which suggested a complex relationship between previous tuberculose infection and the lung cancer. However, data on the treatment of TB in patients with lung cancer still needs further investigation [11].

Against multidrug-resistant tuberculosis (MDR-TB), various azole-type drugs are currently used, such as thioridazine, metronidazole, doxycycline, tigecycline, co-trimoxazole, and a combination of two antimicrobial agents: trimethoprim (TMP) and sulfamethoxazole (SMX) [12]. Despite some success of those drugs against TB, novel chemical entities are still needed in order to develop new alternative drugs [13,14] with improvred efficacy and novel modes of action. In the same vein, new anticancer drugs are developed to support this need based on the libraries of heterocyclic derivatives [15].

In the search for anti-TB compounds based on azo-heterocycles, Joshi et al. [16] reported the synthesis and antitubercular activity (MIC 6.25–100 μg/mL) of pyrrolyl derivatives. They found that some compounds indicate occupation into the hydrophobic pocket of InhA enzyme, thus corroborating that some compounds exhibited inhibition activities against InhA. Two lead compounds displayed a significant activity (6.25 μg/mL) against *M. tuberculosis* H37Rv strain.

Among nitrogen-based biocompounds, the 1,2,3-triazole moiety is an important pharmacophore system which is frequently used as a building block for the discovery of new biological targets [17]. This heterocycle scaffold with three nitrogen heteroatoms can be prepared by click chemistry, via copper(I)-catalyzed alkyne-azide cycloaddition (Cu-AAC) [18]. In general, 1,2,3-triazole derivatives are stable to hydrolysis under acidic or basic metabolic degradation conditions; beyond that, triazoles are weakly acidic or basic. 1,2,3-Triazoles can interact with different biological targets through hydrogen bonding, non-covalent and van der Waals interactions, as well as via dipole-dipole interactions.

The synthesis of oxadiazole derivatives has been explored in order to expand their biological applications, this heterocycle being well known as a peptidomimetic moiety (amide bioisoster), besides esters and carbamates, and this class of compound has a broad-spectrum biological activities [19,20].

The 1,2,4-oxadiazole [20] and 1,2,3-triazole [21] are important small heterocycles used in the design of active molecules, notably in antituberculosis studies (Fig. 1) [20–22]. Phatak et al. [23] describe a series of new indanol-1,2,3-triazole derivatives as new antitubercular agents. Most of these compounds have displayed good antitubercular activity against *M. tuberculosis* H37Rv with MIC values ranging from 6.25 to ≥25 μM, except for one compound with 1.56 μM. In addition, a molecular docking study demonstrated that these compounds show affinity with the active site of Mycobacterial enoyl-ACP-reductase (MtbInhA) enzyme.

Recently, Thanh et al. disclosed a competitive inhibition of the *M. tuberculosis* protein tyrosine phosphatase B (MtbPtpB) by a pyrano-pyrimidine-(1*H*-1,2,3-triazole) D-glucoconjugate **A** (IC_{50} = 1.56 μM) *in vitro* [22]. Analogously, M. Muthukrishnan et al. used click chemistry to prepare a library of spirochromone glycero-1,2,3-triazoles **B** showing strong antimicrobial activity (IC_{50} = 0.78 μg/mL against $H_{37}Rv$ strain) [24]. Following the same approach, Naidu et al. designed various derivatives combining triazole/indole-piperazin-isoxazole which showed improved anti-TB activity specifically compound **C** (MIC = 6.16 μM) against Mtb $H_{37}Rv$ strain and two wild strains isolated from TB patients [25]. The conjugation through formation of an oxadiazole was also performed with 1,2,4-oxadiazole-piperazine-quinoline **D** which showed antitubercular potential against Mtb $H_{37}Rv$ (MIC = 0.25 μg/mL) [19]. In our group, we recently developed a methodology to prepare closely related *N*-cyclohexyl-1,2,4-oxadiazole derivatives **E** and **F** which showed antitumor activity against malignant prostatic cells (PC3, IC_{50} = 13.6 μM) and glioblastoma cancer (SNB19, IC_{50} = 21.7 μM) [26]. Moxifloxacin-acetyl-1,2,3-1*H*-triazole-methyleneisatin hybrids (**G**) were synthesized by Gao et al. as potential anti-tubercular agents against drug-susceptible (MTB H37Rv) with MIC ranging from 0.12 to 16 μg/mL. Two compounds proved to be more active against rifampicin-resistant and multidrug-resistant *M. tuberculosis* strains [27].

Glycoconjugates are an important class of biomolecules and useful scaffolds in drug discovery [28]. Carbohydrate-based heterocycles have been recently used as templates to generate a wide range of bioactive molecules [29,30]. As building block, the carbohydrate moiety allows the synthesis of sugar-based libraries for pharmacological screening, but it also may act as a multifacet prodrug entity, in terms of solubility and site selectivity [30,31]. Having these different aspects in mind, we have recently conjugated a carbohydrate-glycerol moiety to access new 1,2,3-triazole glucoglycerolipid analogues [32].

In medicinal chemistry, hybrid molecules are an interesting concept, where pharmacophore groups are connected in order to produce a more biologically active molecule [33]. In this context, the present work aims at extending our approach to prepare 1,2,3-triazole/1,2,4-oxadiazole hybrid templates of new bioactive chemical entities [19,31,32,34–36]. In this paper, we plan to synthesize glucoglycero and 1,2,3-triazole moieties linked to 1,2,4-oxadiazole *via* copper-catalyzed alkyne-azide cycloaddition (CuAAC) and explore their biological activity against tumor cells and *M. tuberculosis* (Scheme 1).

2. Results and discussion

2.1. Chemistry

2.1.1. Synthesis of the alkynylated 1,2,4-oxadiazole derivatives

We have recently described an efficient method to prepare efficiently 3,5-substituted 1,2,4-oxadiazoles **2a-c,e-h,j-k** under microwave irradiation (Scheme 2) [19]. *Meta*- and *para*-nitrobenzamidoximes were used to prepare the corresponding

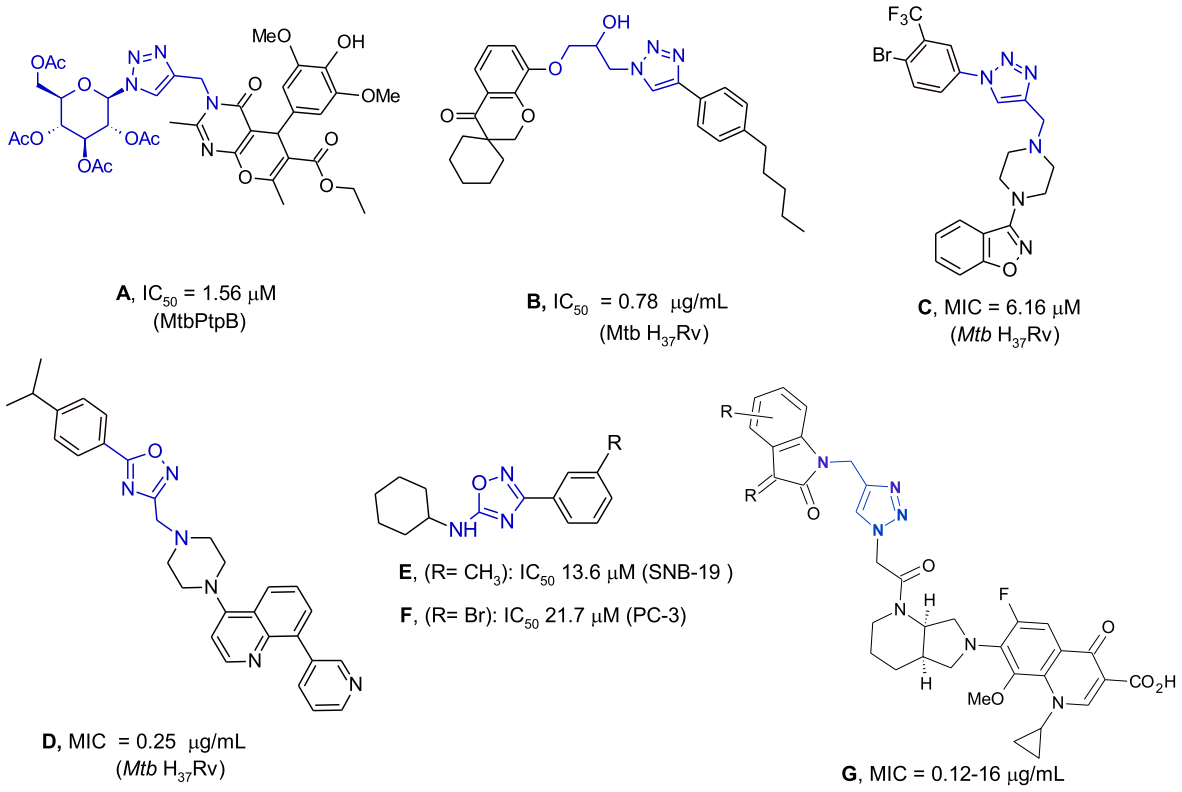

Fig. 1. Recent anti-TB and anticancer compounds containing triazole or oxadiazole scaffolds.

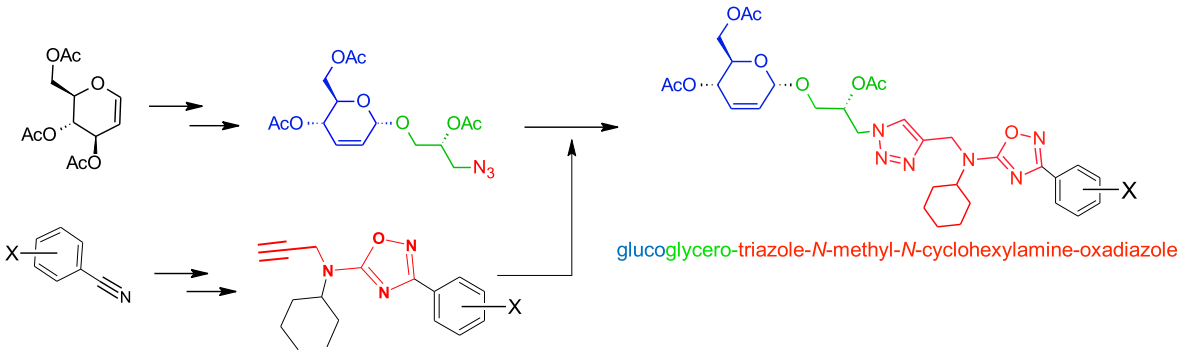

Scheme 1. General strategy for the synthesis of glucoglycero-1,2,3-triazole/1,2,4-oxadiazole derivatives.

oxadiazoles **2d** and **2i** in reasonable yields, 63 and 76%, respectively. Library of heterocycles was extended involving ethynyl- (**1l**) and propargyloxy- (**1m**) benzamidoximes to afford the alkynylated 1,2,4-oxadiazole derivatives **2l** and **2m** in satisfactory yields, 63% and 70%, respectively. The oxadiazole **2m** was obtained in a three-step procedure starting from 4-hydroxybenzonitrile. Alkylation of the phenol group using propargyl bromide/K_2CO_3 in DMF afforded 4-propargyloxybenzonitrile in 95% yield, which was efficiently converted into the corresponding benzamidoxime in 87% yield using hydroxylamine in 1:1 ethanol/water [37]. Reaction with dicyclohexylcarbodiimide (DCC) was carried out in DMF under microwave irradiation [19] to obtain the corresponding 5-cyclohexylamino-1,2,4-oxadiazole **2m** in 80% yield, and an overall yield of 66% for the three steps. Compound **2n** was obtained in 80% yield after reflux in acetic anhydride for 2h.

In a diversity-oriented approach, we considered at this stage the N-alkylation at the amino group in **2a-m**. Optimization of the reaction was first explored on compound **2e** (see Table S1). Following a standard N-alkylation protocol, **2e** was reacted with propargyl bromide (2 equiv) and K_2CO_3 (1 equiv) in DMF at room temperature, but a maximum yield of 31% was reached even after 72 h. Increasing the amounts of base and halide did not result in better yields. Finally, using *tert*-BuOK (1 equiv) as the base with 2 equiv of propargyl bromide made a decisive improvement after 2–4 h reaction, the expected *N*-propargylated derivative **3e** was isolated in 93–95% yields.

With an optimized protocol in hands, we applied these conditions to prepare a library of *N*-propargyl-*N*-cyclohexyl-1,2,4-oxadiazole derivatives. Conversion of **2a-m** gave the corresponding *N*-alkynylated 1,2,4-oxadiazoles **3a-m** in yields ranging from 63 to 95% after chromatography column purification (Table 1). Among the derivatives prepared, **3l** and **3m** were equipped with two

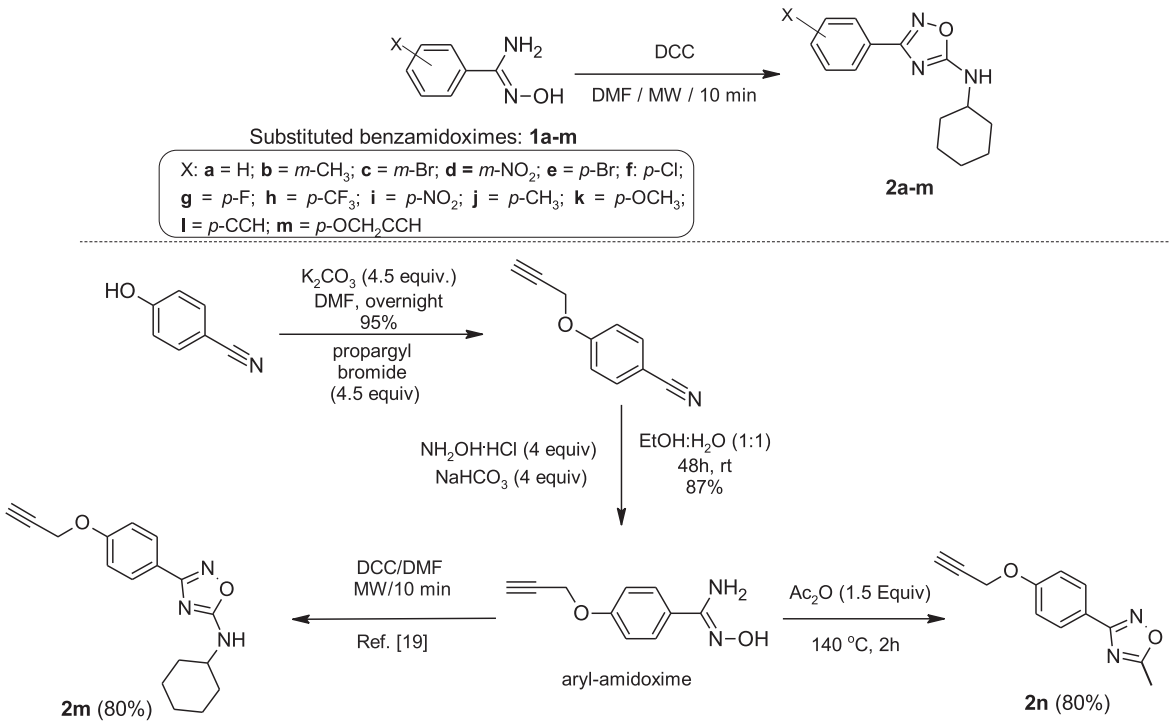

Scheme 2. Synthesis of 3-aryl-1,2,4-oxadiazole **2a-n**.

ethynyl moieties, aiming at further synthesizing bis-triazole compounds.

The structures of synthesized compounds **2a-m** and **3a-m** were assigned by ES-HRMS, and ^{1}H and ^{13}C NMR spectral analysis (see SI). As representative sprectroscopy data, compound **3a** displayed large signals between 1.12 and 2.00 ppm (10H) due to the cyclohexyl CH_2 groups; the triplet of triplets at 3.98 ppm (1H, $J_{ax\text{-}ax} = 11.7$ and $J_{ax\text{-}eq} = 3.5$ Hz) is assignable to the a

-neighbouring cyclohexyl CH. The triplet at 2.27 ppm ($J = 2.4$ Hz) corresponding to the ethynyl H and the CH_2 signal at $\delta = 4.30$ ppm ($J = 2.4$ Hz) confirmed the *N*-alkynylated 1,2,4-oxadiazole structure **3a**. The ^{13}C NMR spectrum showed oxadiazolic carbon signals (168.5 and 170.9 ppm) and the propargyl moiety was characterized by signals at 30.5 ppm (CH_2) and 71.9 and 79.7 ppm (alkynyl carbons).

All the ESI-HRMS of the compounds were dominated by their protonated species. Although the ESI technique was used for exact mass determination, some important fragments could be detected. Compounds **2l** and **2m** showed the expected MH^+ peaks. Additionally, compound **2l** showed MS fragments *m*/*z* 268 (base peak) and *m*/*z* 143 ($C_9H_7N_2$) due to the C5–N^4 and N^2–O cleavages of the oxadiazole ring to form a diaziridine cation (Fig. S1). In general, protonated forms of **2l** or **2m** undergo dissociation via pathway A. Compound **2m** showed MS fragments *m*/*z* 298 (MH^+) and *m*/*z* 173 ($C_{10}H_9N_2O$, base peak); this last one was the major ion, likely because the diazirine cation was stabilized by resonance-donating effect of the *p*-$OCH_2C{\equiv}CH$ substituent (Fig. S1).

On the other hand, the *N*-propargylated 1,2,4-oxadiazoles **3a-m** undergo dissociation via pathway B, by which the neutral diazirine molecule is released, leading to the *m*/*z* 164 peak for all the derivatives (Fig. S1). Compounds **3b**, **3c**, **3f** and **3j** showed heterolytic cleavage of the N–C bond on the propargylic moiety to form the ions *m*/*z* 258, 322, 278 and 258, respectively. In addition, for compounds **3k** and **3m**, an increase of intensity was observed for the *m*/*z* 164 peak. A possible explanation for this abundance is also due to the diazirine cation stabilization by *p*-OCH_3 (**3k**) and *p*-$OCH_2C{\equiv}CH$ (**3m**) substituents, which should favour cleavage to the *m*/*z* 164 fragment (Fig. S1).

2.1.2. Synthesis of glucoglycero-heterocycles based on 1,2,3-triazole and 1,2,4-oxadiazole

The azidosugar **4** was prepared according to our published protocol [32]. The 1,3-dipolar cycloaddition protocol was then applied in reacting **4** with **2l**, **2m** and **3a-m** to furnish a diversity of glucoglycero-heterocyclic systems.

In a first attempt, the reaction was carried out using $CuSO_4{\cdot}5H_2O$/*tert*-BuOH/H_2O and sodium ascorbate as catalytic system to convert **3a** into **5a**; such conditions resulted in low yields (35%), probably due to the low solubility of the reagents. However, the yield was increased when *tert*-butanol was replaced by dichloromethane, employing a 1:1 (v/v) biphasic mixture of CH_2Cl_2:H_2O. Under inert atmosphere, the reaction was completed in 45 min at room temperature and compounds **5a** and **5b** were obtained in 78% and 64% yield, respectively (Table 2). *N*-propargyl-*N*-cyclohexyl-1,2,4-oxadiazoles **3c-k** were similarly reacted with **4** to afford glucoglycero-heterocycles **5c-k** in moderate yields (47–64%) for *meta*-derivatives, and good-to-excellent yields (85–90%) for *para*-substituted derivatives, while no electron-withdrawing or donating effects was observed, see Table 2. The structures of compounds **5a-k** were assigned on the basis of their ^{1}H and ^{13}C NMR spectral analysis, and ESI-HRMS. In the ^{1}H NMR spectrum of compounds **5a-k**, the signal of H-1 (anomeric hydrogen) ranged from $\delta = 4.54$–4.99 ppm as a broad singlet. The vinylic protons H-2 and H-3 showed a chemical shift $\delta = 5.7$–5.9 ppm, with $J_{2,3} = 9.6$–10.6 Hz vicinal coupling. H-5 protons appeared at $\delta = 4.07$–4.11 as a multiplet ddd ($J_{5,4}$; $J_{5,6a}$; $J_{5,6b}$) and remarkable trans diaxial relationship with H-4 ($J_{5,4} = 9.1$–9.9 Hz). These data corroborate with 2,3-dideoxy-α-D-*erythro*-hex-2-enopyranosidic structures. Aditionally, DEPT spectroscopy, COSY, and HSQC were used for complete assignment.

Table 1
Synthesis of the *N*-propargyl-1,2,4-oxadiazole derivatives **3a-m**.

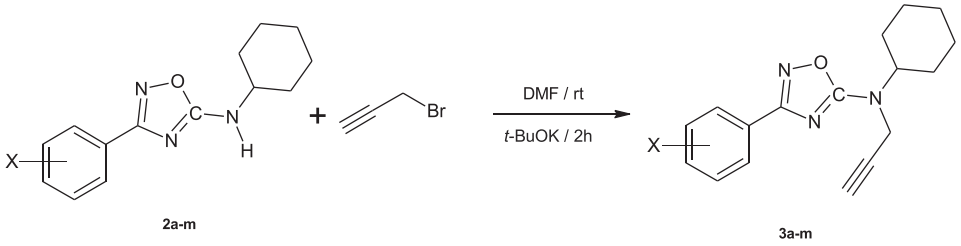

2a-m **3a-m**

3a, 87%

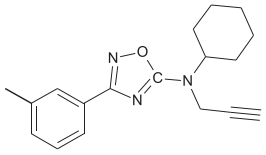

3b, 70%

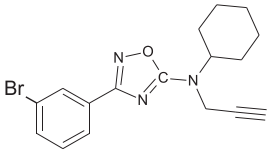

3c, 68%

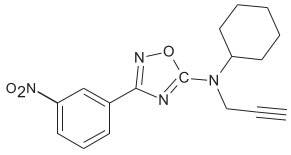

3d, 63%

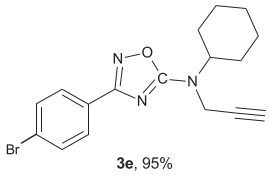

3e, 95%

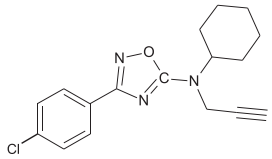

3f, 90%

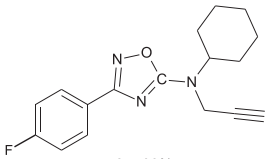

3g, 83%

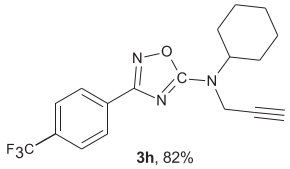

3h, 82%

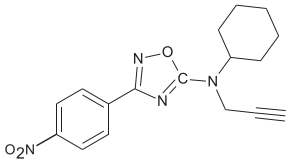

3i, 93%

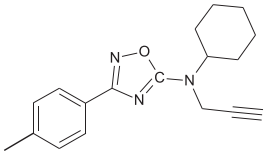

3j, 86%

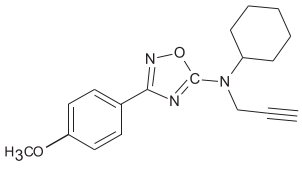

3k, 87%

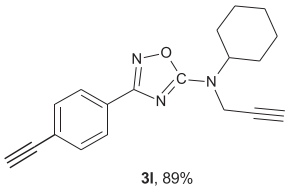

3l, 89%

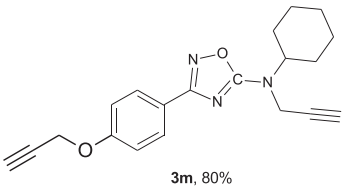

3m, 80%

Yields after chromatography column.

Table 2
Synthesis of glucoglycero-triazole-oxadiazole derivatives **5a-k**.

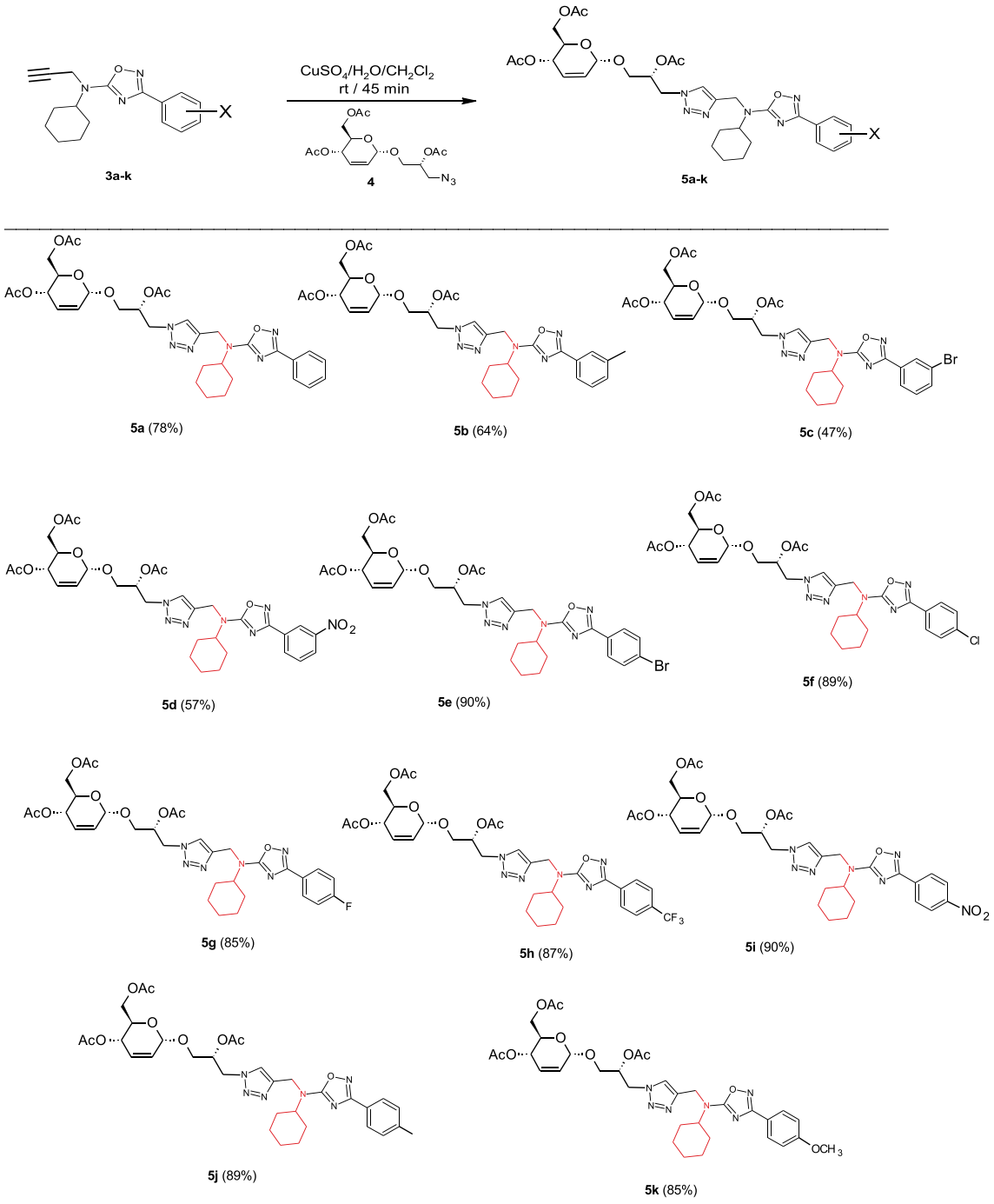

Yields after chromatography column.

Alkynylated 5-amino-1,2,4-oxadiazoles **2l** and **2m** were also reacted with **4** to furnish the new triazole/oxadiazole derivatives **6** and **7** in 91 and 94% yield, respectively (Scheme 3). In the ^{1}H NMR spectrum, the NH protons appeared as a broad doublet at $\delta = 5.18–5.24$ ppm with $J = 8.3$ Hz. The ^{1}H and ^{13}C NMR, and 2D NMR correlation spectroscopy were used for a complete assignment.

To prepare differents glucoglycero derivatives, compounds **8** and **9** were synthesized with 69% and 87% of yields, respectively. In the structure of compound **8** *N*-cyclohexyl group was replaced by methyl group at C-5 carbon position of oxadiazole. Compound **9** represent a derivative without 1,2,4-oxadiazole moiety, and with a long chain of ten-carbons at C-4' position of the triazole.

The azido-sugar **4** was condensed with the bis-alkynes **3l** and

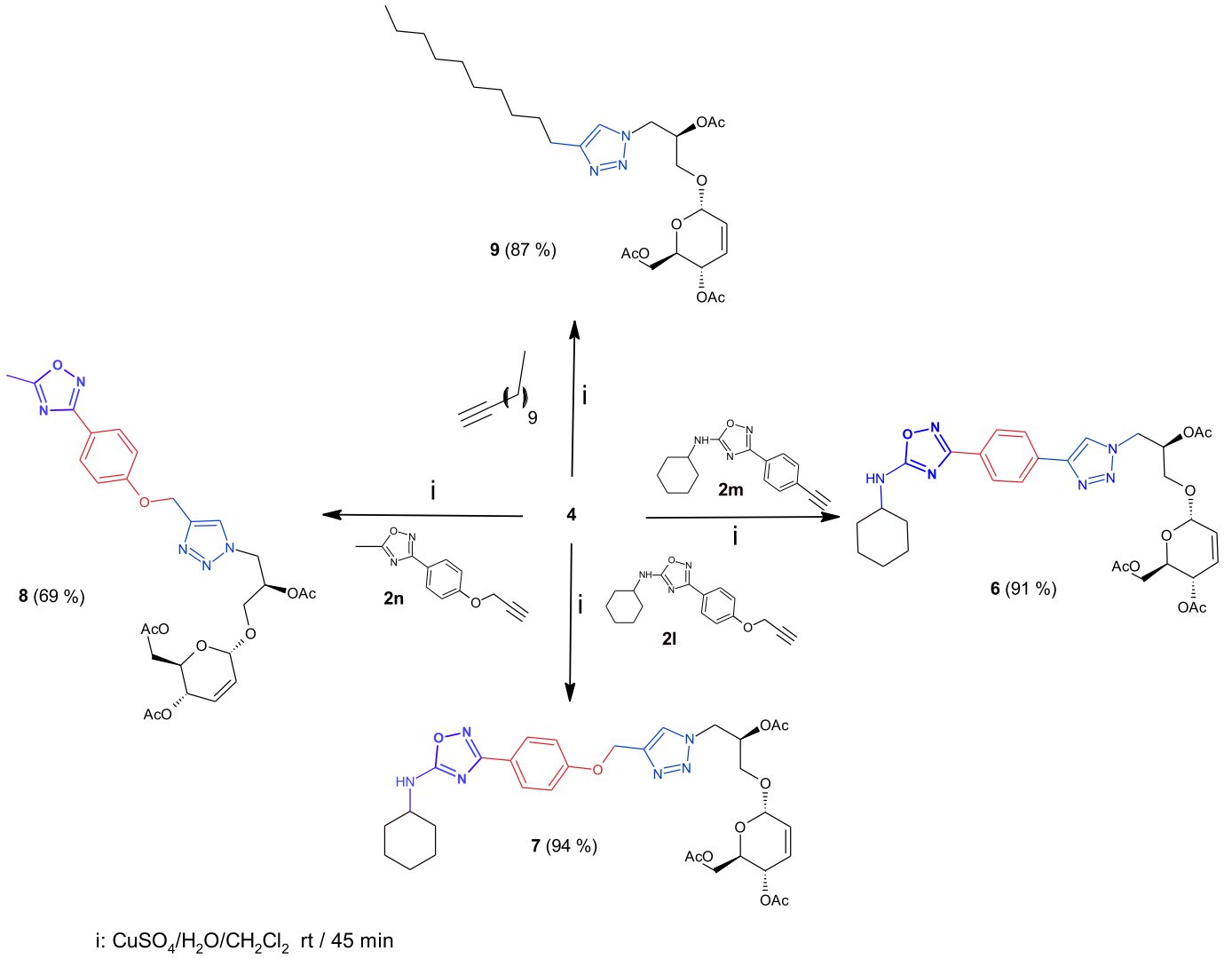

Scheme 3. Synthesis of glucoglycero-triazole derivatives **6**–**9**.

3m to afford in 62 and 67% yield, respectively, two sugar-derived bis-triazoles **10** and **11** (Scheme 4). The ^{1}H and ^{13}C NMR sprectrum revealed the duplicated sugar moieties. In the case of **10** for instance, anomeric protons appeared as two broad singlets at $\delta = 4.98$ and 5.05 ppm and anomeric carbons appeared at $\delta = 94.6$ and 94.7 ppm. The ^{1}H and ^{13}C NMR were used for a complete assignment.

We have thus synthesized a large library of 43 compounds, from which a subfamily of glycoconjugates was developed and tested for their activity against human tumor cell lines as well as for their antitubercular potential.

2.2. Biological evaluation

2.2.1. In vitro antiproliferative activities

Seventeen compounds were selected and tested to verify their cytotoxic potential (at 25 μM concentration) against five tumor cell lines: PC-3 (prostate adenocarcinoma), HCT-116 (colorectal tumor), NCIH 460 (lung carcinoma), SKMEL-103 (melanoma) and AGP-01 (gastric tumor). The compounds were shown to inhibit cell growth, and we focused on those inhibiting above 50% cell proliferation as being qualified for the IC_{50} determination assay (50% inhibitory concentration of cell growth) (Table 3).

We focused our attention on NCIH 460 (lung carcinoma) cells because this cancer represents one of the major public health problems, and there are reports linking lung cancer and tuberculosis infections [11,38]. Data are presented in Fig. 2 as % inhibition of proliferation against NCIH-460, showing cell growth inhibition above 50% at single concentration (25 μM) and in Table 5 as IC_{50} values in μg/mL and μM for compounds **2m**, **3g** and **3k**, after 72 h of treatment as determined by the MTT method. According to Fig. 2 and Table 4, compounds **2m** (17.8 μM), **3g** (3.87 μM) and **3k** (3.21 μM) expressed the best inhibition of proliferation.

Propargylamino derivatives such as pargyline and rasagiline are known for their activity against human breast tumors [39] and against Parkinson's disease [40]. Pargyline is a monoamine oxidase (MAO) inhibitor, which prevents the activity of lysine-specific demethylase 1 (LSD_1), an overexpressed enzyme in breast cancer. Another mechanism of action may be related to substances containing a 1,2,4-oxadiazole moiety, that have already been reported as apoptosis inducers in cancer cell strains. Such compounds act by activating the caspase pathway, leading to proteolytic degradation and programmed cell death [41]. Although mechanistic studies could not be performed so far, it is possible that compounds **3g** and **3k** might act in the same way.

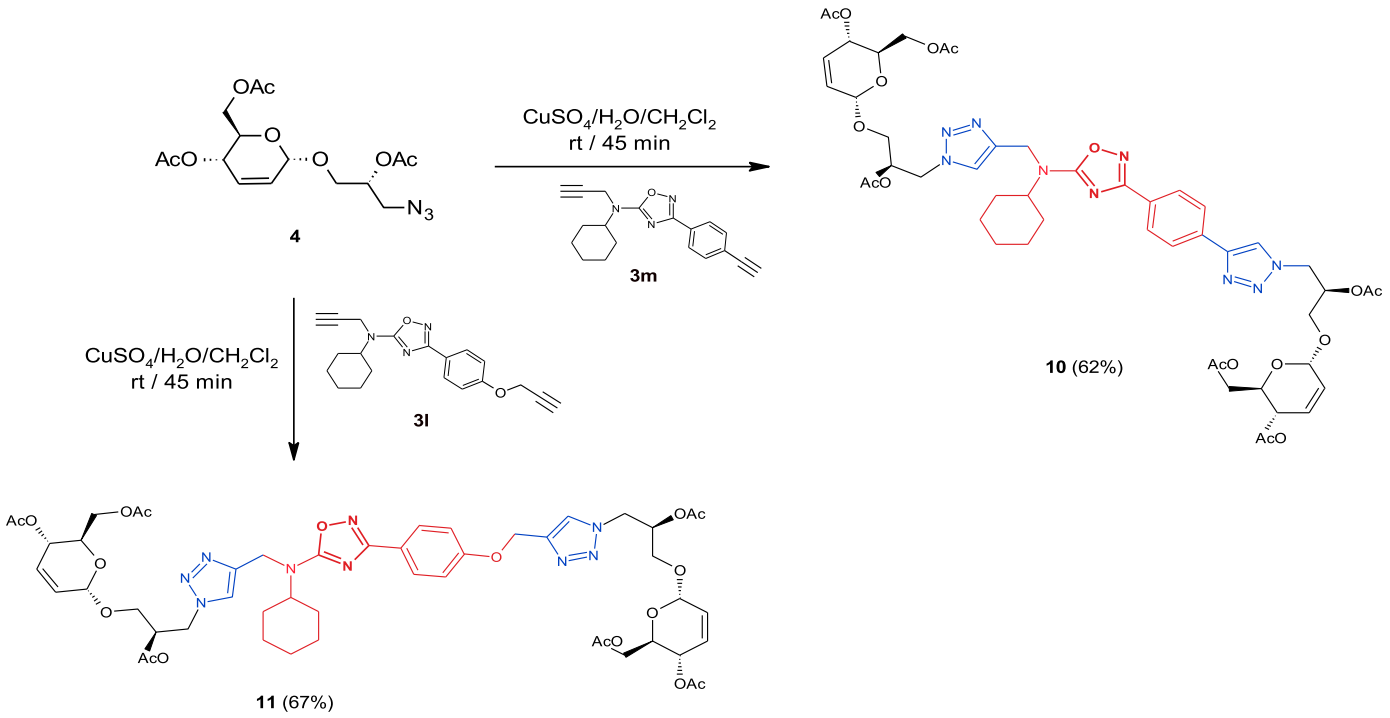

Scheme 4. Synthesis of bis-1,2,3-triazoles **10** and **11**.

Table 3
Percentage of inhibition of cellular proliferation of the compounds (25 μM) after 72 h determined by the MTT method.

Compounds	SKMEL-103	AGP-01	HCT-116	PC-3	NCIH-460
2d	32.0 ± 0.09	11.6 ± 0.22	14.1 ± 0.14	9.9 ± 0.25	n.d.
2i	50.7 ± 0.15	53.2 ± 0.03	n.d.	20.3 ± 0.19	10.4 ± 0.14
2l	40.1 ± 0.28	44.4 ± 0.58	60.7 ± 0.01	46.0 ± 0.08	34.0 ± 0.40
2m	62.8 ± 0.50	2.6 ± 0.25	43.3 ± 0.49	64.2 ± 0.42	**75.7 ± 0.55**
3a	28.6 ± 0.10	47.0 ± 0.14	n.d.	23.7 ± 0.54	22.6 ± 0.40
3b	87.7 ± 0.04	94.5 ± 0.04	86.5 ± 0.18	29.4 ± 0.26	40.2 ± 0.38
3c	39.4 ± 0.12	69.1 ± 0.23	65.6 ± 0.22	58.6 ± 0.09	17.9 ± 0.26
3d	44.4 ± 0.39	46.0 ± 0.18	24.8 ± 0.27	7.2 ± 0.02	5.8 ± 0.14
3g	47.3 ± 0.34	50.4 ± 0.56	44.9 ± 0.43	25.4 ± 0.07	**50.5 ± 0.86**
3i	18.5 ± 0.08	52.5 ± 0.13	37.2 ± 0.26	53.7 ± 0.28	n.d.
3k	37.3 ± 0.42	57.3 ± 0.35	40.7 ± 0.14	23.7 ± 0.54	**69.1 ± 0.12**
5b	69.0 ± 0.26	38.9 ± 0.25	69.5 ± 0.04	9.2 ± 0.05	26.1 ± 0.60
5c	52.3 ± 0.05	59.9 ± 0.04	n.d.	45.5 ± 0.43	27.1 ± 0.15
5d	42.2 ± 0.07	44.7 ± 0.12	27.7 ± 0.09	38.4 ± 0.27	n.d.
5g	20.7 ± 0.12	69.4 ± 0.22	44.9 ± 0.43	7.1 ± 0.11	17.7 ± 0.48
5i	30.6 ± 0.06	47.6 ± 0.22	39.1 ± 0.10	28.8 ± 0.08	36.3 ± 0.21
5k	29.8 ± 0.24	59.2 ± 0.37	24.2 ± 0.01	21.6 ± 0.20	24.2 ± 0.24

*The best results are highlighted in bold; n.d. = not determined.

2.2.2. *In vitro antimycobacterial activity*

In continuation, all new compounds were screened against *M. tuberculosis* H37Rv (ATCC 27294) and *M. tuberculosis* H37Ra (ATCC 25177) strains. The minimum inhibitory concentration (MIC) was determined (μg/mL), rifampicin and ethambutol being used as standard compounds. The MIC results of the synthesized compounds along with reference drugs are reported in Table 5.

Cytotoxicity was initially evaluated against two different mammalian cell lines (Raw 264.7 and HepG2) by MTT assay [42,43]. In in vitro screening studies of compounds against *Mycobacterium tuberculosis*, it is common to use different cell lines, such as Raw 264.7 (ATCC TIB - 71) murine macrophages cells and HepG2 cells, as demonstrated in different scientific studies [44–46]. Murine macrophage Raw 264.7 cell line is normaly used for initial bioactivity screening of compounds and predict potential effect in vivo [47]. HepG2 cell lines is a well recognized model system, frequently employed to evaluate liver cell function *in vitro*. The liver is the main organ involved in metabolism, then HepG2 liver cell lines are often used as tools to screen toxicity from test compounds and may thus serve as a useful model [48].

Compounds **2l, 2m** and **3a-m** showed low activity against *M. tuberculosis* (Table 5). However, some derivatives from series **5** and compound **7** produced good antimycobacterial activity against TB (*Mtb* H_{37}Rv). Compounds **5e** and **7** induced particularly good effect with MIC = 8 μg/mL (10 μM) and 16 μg/mL (23.9 μM), respectively, and considering the selective index (Table 6). In general, glycerosugars functionalized with 1,2,3-triazole/1,2,4-oxadiazole moieties were active (**5a**, **5e**, **5j**, **5k**, and **7**); in contrast, larger molecules such as **10** and **11** proved to be unactive against TB. These results agree with the importance of finding small molecules at a lower cost to encourage the development of drugs for the treatment of tuberculosis [49].

Compounds **8** and **9** showed low activities, perhaps this may indicate that the presence of 1,2,4-oxadiazole nucleus and *N*-cyclohexyl group were an important fact to increase the anti-TB activity of glucoglycero-triazole-*N*-cyclohexyl-oxadiazole derivatives and should be considered in future designs of new chemical entities with anti-TB potential.

In general, the lipophilicity of a molecule impacts on the capacity of transmembrane diffusion of a drug, and in case of action against tuberculosis it can inhibit lipid biosynthesis. To understand if there are lipophilic effects from the tested compounds, logP was calculated (see Table 5). We observed, despite moderate-to-low activity against Mtb, that the series of compounds **3a-m** was active when logP was above 4.5, except for compound **3j**; and negligible activity when logP <4.5. On the other hand, from series **5** no indication of correlation with logP was found.

Despite inhibitory activities against Mtb H37Rv observed in series **5**, some of the active compounds presented toxicity in Raw

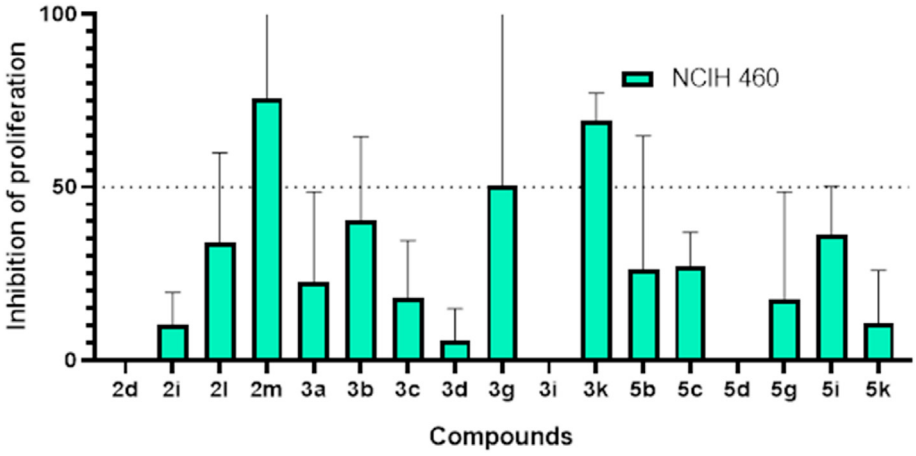

Fig. 2. Percentage of inhibition of proliferation of the compounds against NCIH-460 ($0.1x10^6$ cells/mL) after 72 h.

Table 4
IC_{50} values in μg/mL and μM for compounds **2m**, **3g** and **3k** against NCIH-460.

Compounds	2 m	3g	3k	doxorubicine
Structure	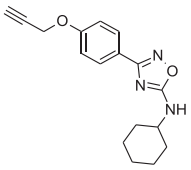	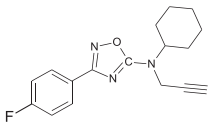	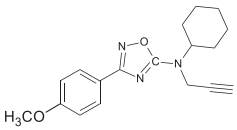	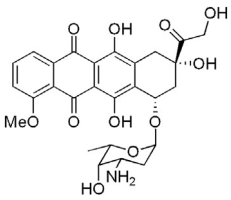
IC_{50} (μg/mL)	5.30	1.16	1.00	0.08
IC_{50} (μM)	17.82 ± 1.8	3.87 ± 0.40	3.21 ± 0.70	0.15 ± 0.02

264.7 and HepG2 cells. In order to learn more about their cytotoxicity, CC_{50} (μM) of selected compounds was evaluated for Vero cells, which are derived from African green monkey kidney. Compounds **5a** (606.8 μM), **5h** (706.3 μM), **5j** (498.3 μM), and **5k** (575.0 μM) were shown to have low cytotoxicity in Vero cells. The selective index (7.9–24.7) can be seen in Table S2.

In recent years, a few articles have made significant strides towards the synthesis of new anti-TB compounds [16,17,21–27,50]; however, there remain important gaps in research on the discovery of a new chemical entity against a new/old drug target.

2.3. Structure activity relationship (SAR) for anti-TB compounds

From the structure of 1,2,4-oxadiazoles structural modification were made. First, N-alkylation made available alkynylated 1,2,4-oxadiazole derivatives with no activity or moderate. Some SAR observations from anti-TB data can be deduced (Fig. 3).

i) In the serie **3** compounds with logP >4.5 (**3b,c,e,f,h**) have moderate activity anti-TB, except for **3j**; and compounds with logP < 4.5 (**3a,d,g,i,k,l,m**) were no effective against Mtb. In general, when we look at Table 5, the data suggest that these compounds were more potent against TB, when their logP ranges from 3.9 to 4.9 (exception **2m**), but not higher or lower. On the other hand, logP in this range does not guarantee an attractive anti-TB activity, e.g. **5g-i.**
ii) Small molecules containing the 1,2,4-oxadiazole scaffold linked to a triazole-glycerosugar possess anti-TB activity, various derivatives **5a**, **5e**, **5j** and the compound **7** showing antimycobacterial activity against *Mtb* $H_{37}Rv$;
iii) Compound **7** was more potent than compound **6**, which may which may suggest that structure 7 is influenced by conformational factors that can potentiate anti-TB activity;
iv) Compound **8** shown to be inactive; probably caused by the absence of the *N*-cyclohexyl group and too low lipophilicity (logP = 2.34);
v) Compound **9**, glucoglycerol-triazole derivative, was no active for TB; this can indicate that 1,2,4-oxadiazole moiety is important for the activity anti-TB;
vi) Large molecules such as **10** and **11** proved to be inactive against TB.

2.4. Molecular docking

Two proteins mycobacterial Enoyl-[acyl-carrier-protein] reductase, InhA (PDB ID: 2NSD) and Decaprenylphosphoryl-beta-D-ribose oxidase, DprE1 (PDB ID: 5OEQ) have recently attracted enough attention for being potential target for growth inhibition of the pathogens. Due to the availability of crystal structure for these two proteins, several reports have demonstrated the potential of the triazole scaffold to inhibit InhA and DprE1 enzymes [51,52] and 1,2,4-oxadiazole inhibits InhA enzyme [53]. Anti-tubercular activity displayed by compounds **5e** and **7** inspired us to perform *in-silico* studies to identify their binding affinity towards InhA and DprE1 protein targets of *M. tuberculosis.* Both proteins were analyzed for its stereo-chemical geometry by procheck Ramachandran plot where DprE1 and InhA has 0% and 0.9% outlier residues, respectively (Table 6: entries 1 and 2; Fig. S2).

Molecular docking analysis revealed that compound **5e** interacts

Table 5
In vitro antimycobacterial activities of the target compounds **2**–**11** expressed as MICs (μg/mL).

Compd	Mol. Wt	logP[a]	Strain (MIC, μg/mL)		CC_{50} (μg/mL)		SI (CC_{50}/MIC)	
			$H_{37}Ra$	$H_{37}Rv$	RAW 264.7	HepG2	(CC_{50}Raw/MIC-$H_{37}Rv$)	(CC_{50}HepG2/MIC-$H_{37}Rv$)
2l	267.32	3.91	32	32	19.82	54.20	0.62	1.69
2m	297.15	3.46	32	32	38.28	118.70	1.29	3.70
4	371.34	1.52	≥64	≥64	106.3	>200	1.66	3.12
3a	281.35	4.10	≥64	≥64	32.13	108.60	0.50	1.69
3b	295.38	4.52	≥64	32	25.89	44.38	0.80	1.38
3c	360.25	4.88	≥64	32	31.77	53.45	0.90	1.67
3d	326.35	4.03	≥64	≥64	34.18	45.48	0.53	0.71
3e	360.25	4.91	32	32	15.67	101.80	0.48	3.18
3f	315.80	4.78	32	**16**	15.12	41.26	0.95	2.58
3g	299.34	4.26	64	64	20.92	41.08	0.32	0.64
3h	349.35	4.99	64	32	38.32	61.89	1.20	1.93
3i	326.35	4.06	≥64	≥64	26.74	43.73	0.41	0.68
3j	295.38	4.55	64	≥64	17.57	91.93	0.27	1.43
3k	311.38	4.16	≥64	64	27.96	72.54	0.46	1.13
3l	305.37	3.86	nd	≥64	13.11	27.95	0.20	0.43
3m	335.40	4.32	≥64	64	100.7	>200	1.57	3.12
5a	652.69	3.99	**16**	**16**	28.61	19.91	1.78	1.24
5b	666.72	4.42	≥64	≥64	46.38	39.20	0.72	0.61
5d	697.69	3.93	≥64	≥64	100.4	>200	1.56	3.12
5e	731.59	4.80	**4**	**8**	39.11	47.63	**4.89**	**5.95**
5f	687.14	4.67	64	64	35.54	46.91	0.55	0.73
5g	670.68	4.16	≥64	≥64	31.48	28.80	0.49	0.45
5h	720.69	4.89	≥64	≥64	64.11	81.40	1.00	1.67
5i	697.69	3.95	≥64	≥64	80.22	>200	1.25	3.12
5j	666.72	4.44	**8**	**16**	45.32	36.78	2.83	2.30
5k	682.72	4.05	**16**	32	86.32	141.20	2.70	4.41
6	638.67	3.78	≥64	≥64	16.29	79.84	0.25	1.24
7	668.69	4.00	**16**	**16**	33.28	99.46	2.08	**6.21**
8	585.57	2.34	≥64	≥64	111.8	37.67	1.74	0.58
9	537.65	5.24	64	64	30.37	59.05	0.47	0.92
10	1048.06	–	≥64	≥64	116.70	11.79	1.82	0.18
11	1078.08	–	≥64	≥64	>200	47.02	3.12	0.73
RIF	822.94	2.67	0.062	0.125	80.39	175.90	643.12	1407.20
EMB	204.31	0.35	1	1	>400	>400	400	400

The best results are highlighted in bold; RIF: Rifampicin; EMB: Ethambutol.
[a] The logP was calculated using the Molinspiration molecular property (http://www.molinspiration.com). The SMILES notation was generated in ACD/ChemSketch (version 12.0) and input in molinspiration program.

Table 6
Number of amino acid residues and their percentage in favored, additional allowed, additional generously allowed, and outlier region of Ramachandran plot for both DprE1 and InhA proteins in complex with compounds **5e** and **7**.

Entry	Protein complexes	Most favored region	Additional allowed region	Generously allowed region	Disallowed region
1	DprE1	325 (91%)	32 (9%)	0 (0.0%)	0 (0.0%)
2	InhA	209 (92.9%)	13 (5.8%)	1 (0.4%)	2 (0.9%)
3	DprE1-**5e** complex	292 (81.8%)	60 (16.8%)	4 (1.1%)	1 (0.3%)
4	DprE1-**7** complex	295 (82.6%)	56 (15.7%)	5 (1.4%)	1 (0.3%)
5	InhA-**5e** complex	195 (86.7%)	29 (12.9%)	1 (0.4%)	0 (0.0%)
6	InhA-**7** complex	192 (85.3%)	30 (13.3%)	1 (0.4%)	2 (0.9%)

with binding site residues of DprE1 protein (Dscore, −5.205 kcal/mol; ΔG° −99.55 kcal/mol) *via* H-bond (Gly_55, Gly_117, Lys_418) and pi-pi interaction (His_132). In case of InhA-**5e** complex, compound **5e** showed interactions with binding site residues of InhA protein (Dscore, −2.094; ΔG° −108.47 kcal/mol) *via* H-bond (Ser_20, Ala_22) as depicted in Fig. 4a and b (Table 7: entries 1 and 2). Likewise, compound **7** interacts with binding site residue of DprE1 protein (Dscore, −1.763 kcal/mol; ΔG° −123.82 kcal/mol) through H-bonds (Ser_59, Try_60, Gly_117, Lys_418, Tyr_415) and pi-pi interaction (Tyr_415). Compound **7** showed interactions with the binding site residue of InhA protein (Dscore, −3.464 kcal/mol; ΔG° −87.30 kcal/mol) through H-bond (Ser_20, Met_98) as shown in Fig. 4c and d (Table 7: entries 3 and 4).

Next, MD simulations were performed to evaluate the stability of these complexes in he binding site. Post simulations, all the four complexes displayed good structural geometry without any significant outlier residues (Figs. S2c–f; Table 6: entries 3–6).

During simulation, compound **5e** had average RMSD of 3.02 Å and 1.44 Å in complexed with InhA and DprE1 proteins, respectively (Figs. S3a and S3b). On other side, compound **7** complexed with InhA and DprE1 revealed the average RMSD of 2.05 Å and 2.09 Å, respectively (Figs. S3c and S3d). These compounds showed fluctuations in the acceptable range (3 Å). The histogram plot depicted in Fig. S4, showed the nature of interaction between ligand and protein during MD simulation where ligand interacted to the residues by H-bond (green), salt bridge (pink), water bridge (blue), and hydrophobic interaction (grey). For InhA-**5e** complex, benzyl moiety-maintained pi-pi interaction with Phe_41 for at least 39% of the simulation time (Fig. S4a). The oxygen atom of acetic acids-maintained H-bond with Ala_22 and Ile_194 by 98% and 73%

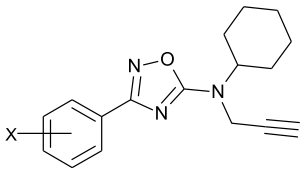

logP < 4.5	logP > 4.5
no activity >/= 64 μg/mL	moderate activity 16-32 μg/mL
X = H, *m*-NO_2, *p*-NO_2, *p*-F, *p*-OMe, *p*-*CCH*, *p*-OCH_2CCH	X= *m*-CH_3, *m*-Br, *p*-Br, *p*-Cl (**50.6 μM**), *p*-CF_3

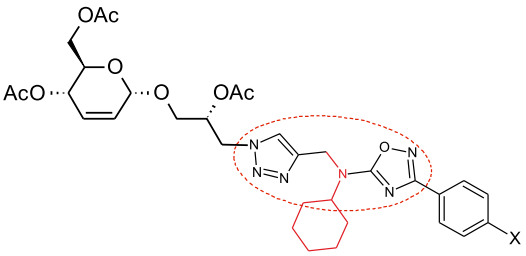

Glucoconjugates: oxadiazole-triazole hybrids

5a (X= H, 24.5 μM), **5e** (X= Br, 10.9 μM), **5j** (X= CH_3, 24 μM) and **5k** (X= OCH_3, 46.9 μM)

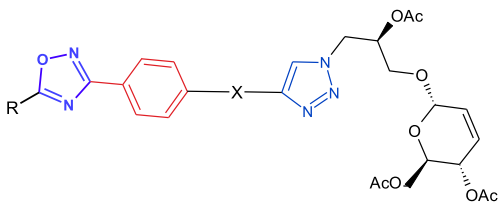

6: X = no spacer (≥ 64 μM); R = HN-cyclohexyl

7: X = OCH_2 (23.9 μM); R = HN-cyclohexyl

8: X = OCH_2 (≥ 64 μM); R = CH_3

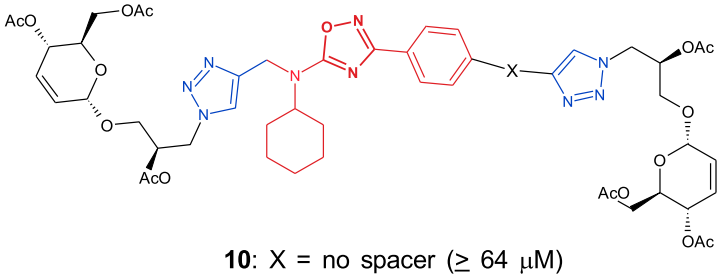

10: X = no spacer (≥ 64 μM)
11: X = OCH_2 (≥ 64 μM)

Fig. 3. Structure-activity relationship for anti-TB compounds.

of the simulation time, respectively. For DprE1-**5e** complex, 1,2,3-triazole maintained H-bond and pi-pi interaction to the residues Gly_117 and His_132 by 37% and 34%, respectively (Fig. S4b). The oxygen atom of acetic acid and nitrogen atoms of *N*-cyclohexyl-1,2,4-oxadiazol displayed various interactions as shown in Figs. S4c and d. Both the compunds **5e** and **7** showed interactions with several common residues in complex with both InhA and DprE1 proteins. While MD simulation process, compound **5e** and **7** were always bounded with 8−10 and 10−12 contacts with binding site residues of InhA protein (Figs. S5a and S5b). Similarly, compound **5e** and **7** were always bounded with 5−7 and 10−12 contacts with binding site residues of DprE1 protein during MD simulations (Figs. S5c and S5d).

3. Conclusion

We have developed protocols to prepare a library of thirty new compounds applying CuAAC and N-alkylation. Among the various molecules, *N*-propargyl-1,2,4-oxadiazoles **3g** and **3k** exhibited the best antiproliferative activities *in vitro* against NCIH-460 (lung carcinoma). Glycerosugars conjugated to 1,2,4-oxadiazole via a 1,2,3-triazole linkage (**5a**, **5e**, **5j** and **7**) showed *in vitro* inhibitory activity on the level IC50 < 24.5 μM against *M. tuberculosis* (*Mtb* H_{37}Rv). In general, the data suggest that these compounds were more potent against TB, when their logP ranges from 3.9 to 4.9. On the other hand, logP in this range does not guarantee an attractive anti-TB activity. The largest molecules bis-triazoles **10** and **11**, proved inactive against TB. In contrast, glucoglycero-triazole-oxadiazoles **5e** (10 μM) and **7** (23.9 μM) were the most active with the best selectivity index. In addition, molecular docking study for the most active compounds (**5e** and **7**) against *M. tuberculosis* was established for Mtb DprE1 and InhA enzymes. MD simulation carried out at 100 ns supported that both the compounds **5**e and **7** complexed with proteins DprE1 and InhA have stable interactions. Also, RMSD plots indicated both the compounds showed fluctuations in the acceptable range, suggesting their stability within the binding pocket of both the proteins. We thus have found promising hits for the development of new lead compounds against NCIH-460 and tuberculosis. Further development of this new family of compounds is ongoing and will be published in due course.

4. Experimental section

4.1. Chemistry

Melting points were determined in a capillary tube and performed with a PFM II BioSan instrument. HRMS analyses were performed on a Micromass LC-ESI-TOF at the ICOA (Université d'Orléans, France). NMR spectra were obtained with Varian Unity Plus-300 or 400 spectrometers using CDCl3 as solvent and calibrated for the solvent signal. Optical rotations were measured using

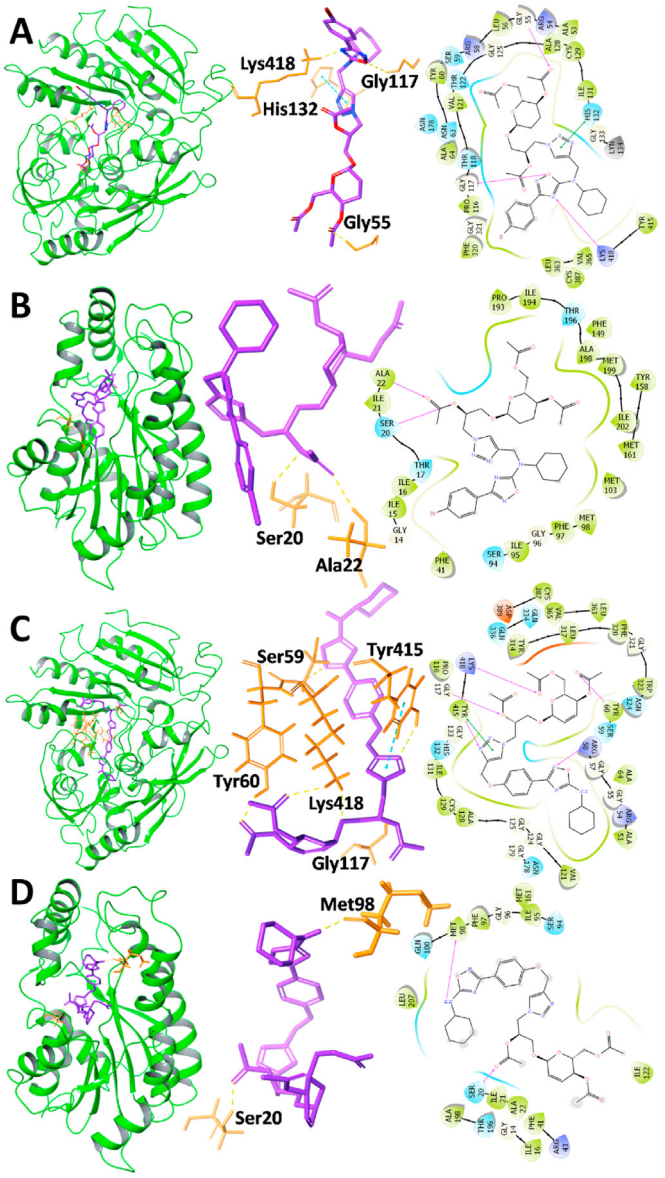

Fig. 4. 3D and 2D interaction poses of compounds to the binding site residue of target proteins [InhA (PDB ID: 2NSD); (PDB ID: 5OEQ)]. A) DprE1-**5e**; B) InhA-**5e**; C) DprE1-**7**; and D) InhA-**7**.

Table 7
Docking score and ΔG° (kcal/mol) for molecules 5e and 7.

Entry	Protein	Ligand	D Score (kcal/mol)	ΔG° (kcal/mol)
1	DprE1	**5e**	−5.205	−99.55
2	InhA	**5e**	−2.094	−108.47
3	DprE1	**7**	−1.763	−123.82
4	InhA	**7**	−3.464	−87.30

a Anton Paar Model MCP200 polarimeter (Na-D-line 589 nm) with a path length of 1 dm. Purifications were performed by column chromatography on Merck silica gel 60 (70–230 mesh). The arylamidoximes **1a-m** were either prepared according to the conventional protocol or by using ultrasound energy [54]. 4-(Prop-2-yn-1-yloxy)benzonitrile [RN 33143-80-5] was prepared by conventional alkylation. *N′*-Hydroxy-4-(prop-2-yn-1-yloxy)benzimidamide [RN 2241224-25-7] was synthesized according to literature process [37]; this arylamidoxime was used as starting material to prepare the oxadiazole **2m** [19].

*4.1.1. Synthesis of 3-aryl-5-cyclohexylamino-1,2,4-oxadiazole derivatives **(2a-n)***

The literature protocol was applied [19].

*4.1.1.1. N-Cyclohexyl-3-(4-ethynylphenyl)-1,2,4-oxadiazol-5-amine (**2l**).* Yield 63% (168 mg), colorless solid; mp 131–133 °C. R_f 0.7 (Hexane-EtOAc, 7:3). ^{1}H NMR (300 MHz) δ 1.15–1.50; 1.61–1.81; 2.07–2.12 (m, 10H, cyclohexyl), 3.18 (s, 1H, CH), 3.66–3.72 (m, 1H, CH cyclohexyl), 5.28 (d, 1H, J = 8.2 Hz, NH), 7.55–7.58 (m, 2H, H_{Ar}), 7.95–7.98 (m, 2H, H_{Ar}). ^{13}C NMR (75 MHz) δ 24.6, 25.3, 33.2, 52.9, 78.9, 83.2, 124.4, 127.1, 127.9, 132.3, 167.8, 170.6. ESI-HRMS calcd for $C_{16}H_{17}N_3O$ $[M+H]^+$: 268.1445; found: 268.1444.

*4.1.1.2. N-Cyclohexyl-3-[4-(prop-2-yn-1-yloxy)phenyl]-1,2,4-oxadiazol-5-amine (**2m**).* Yield 70% (208 mg), colorless solid; mp 119–121 °C; R_f 0.6 (Hexane-EtOAc, 7:3). ^{1}H NMR (300 MHz) δ 1.19–1.49; 1.61–1.68; 1.73–1.8; 2.05–2.12 (m, 10H, cyclohexyl), 2.54 (t, 1H, J = 2.3 Hz, CH), 3.65–3.73 (m, 1H, CH cyclohexyl), 4.74 (d, 2H, J = 2.3 Hz, CH_2), 5.26 (d, 1H, J = 8.2 Hz, NH), 7.01–7.05 (m, 2H, H_{Ar}), 7.92–7.97 (m, 2H, H_{Ar}). ^{13}C NMR (75 MHz) δ 24.6, 25.3, 33.2, 52.8, 55.8, 75.8, 78.1, 115.0, 121.1, 128.7, 159.4, 168.0, 170.4. ESI-HRMS calcd for $C_{17}H_{20}N_3O_2$ $[M+H]^+$: 298.1555; found: 298.1549.

*4.1.1.3. Synthesis of 5-methyl-3-[4-(prop-2-yn-1-yloxy)phenyl]-1,2,4-oxadiazole (**2n**).* In a 25 mL flask, 190 mg (1 mmol) of arylamidoxime and 153 mg (1.5 mmol) of acetic anhydride were added. The mixture was kept under magnetic stirring, at 140 °C, for 2 h. At the end of the reaction, an acid-base extraction was carried out, using a saturated solution of $NaHCO_3$ and ethyl acetate. The product was obtained after crystallization from methanol-water.

Yield 90% (117.5 mg); colorless crystal; mp 53–55 °C; R_f = 0.8 (Hexano/EtOAc, 1:1). ^{1}H NMR (300 MHz): δ 2.55 (t, 1H, J = 2.4 Hz, C≡C<u>H</u>), 2.63 (s, 3H, CH_3),4.75 (d, 2H, J = 2.1 Hz, CH_2), 7.04–7.09 (m, 2H, H_{Ar}), 8.00–8.05 (m, 2H, H_{Ar}). ^{13}C NMR (75 MHz): δ 12.4 (CH_3), 55.8 (<u>C</u>H_2OAr), 75.9 (C≡C), 78.0 (C≡C), 115.2 (2C_{Ar}), 120.2 (C_{Ar}), 128.9 (2C_{Ar}), 159.7 (C_{Ar}), 168.0 (C-oxad), 176.3 (C-oxad).

*4.1.2. Synthesis of 3-aryl-N-cyclohexyl-N-(prop-2-yn-1-yl)-1,2,4-oxadiazol-5-amines (**3a-m**)*

Oxadiazoles **2a-m** (0.5 mmol) were dissolved in dry DMF (0.5 mL), followed by addition of potassium *tert*-butoxide (1 equiv). Then, propargyl bromide (2 equiv) was added and the mixture was stirred at room temperature for 2 h. The reaction mixture was filtered, washed with dichloromethane-water and the solvents were evaporated under reduced pressure. The products were purified by column chromatography using hexane and dichloromethane (2: 8).

*4.1.2.1. N-Cyclohexyl-3-phenyl-N-(prop-2-yn-1-yl)-1,2,4-oxadiazol-5-amine (**3a**).* Yield 87% (122 mg), colorless solid; mp 112–115 °C; R_f 0.4 (hexane-CH_2Cl_2, 1:1). ^{1}H NMR (300 MHz) δ 1.11–1.26, 1.34–1.50, 1.65–1.78, 1.87–2.01 (m, 10H, cyclohexyl), 2.27 (t, 1H, J = 2.4 Hz, CH), 3.98 (dd, 1H, $J_{ax\text{-}ax}$ = 11.7 and $J_{ax\text{-}eq}$ = 3.5 Hz, N–CH), 4.30 (d, 2H, J = 2.4 Hz, CH_2), 7.42–7.48 (m, 3H, H_{Ar}), 8.01–8.04 (m, 2H, H_{Ar}). ^{13}C NMR (75 MHz) δ 25.3, 25.7 (2C), 30.5 (2C), 34.5, 59.0, 71.9, 79.7, 127.3 (2C), 127.8, 128.5 (2C), 130.6, 168.5, 170.9. ESI-HRMS calcd for $C_{14}H_{19}N_3O$ $[M - C_3H]^+$: 244.1414; found: 244.1414.

*4.1.2.2. N-Cyclohexyl-3-(3-methylphenyl)-N-(prop-2-yn-1-yl)-1,2,4-oxadiazol-5-amine (**3b**).* Yield 70% (104 mg), colorless oil; R_f 0.8 (Hexane-CH_2Cl_2, 2:8). ^{1}H NMR (300 MHz) δ 1.11–1.26, 1.35–1.50, 1.65–1.78, 1.86–2,01 (m, 10H, cyclohexyl), 2.27 (t, 1H, J = 2.3 Hz,

CH), 2.42 (s, 3H, CH_3), 3.99 (dddd, 1H, $J_{ax\text{-}ax}$ = 11.8 Hz and $J_{ax\text{-}eq}$ = 3.5 Hz, N–CH), 4.30 (d, 2H, J = 2.3 Hz, CH_2), 7.26 (d, 1H, J = 7.6 Hz, $H_{p\text{-}oxadiazole}$), 7.33 (dd, 1H, J = 7.6 and 7.0 Hz, $H_{m\text{-}oxadiazole}$), 7.82 (m, 2H, $H_{o\text{-}oxadiazole}$). ^{13}C NMR (75 MHz) δ 21.3, 25.3, 25.7 (2C), 30.5 (2C), 34.4, 59.0, 71.9, 79.7, 124.4, 127.6, 127.8, 128.4, 131.4, 138.2, 168.6, 170.8. ESI-HRMS calcd for $C_{18}H_{22}N_3O$ $[M+H]^+$: 296.1763; found: 296.1758.

*4.1.2.3. 3-(3-Bromophenyl)-N-cyclohexyl-N-(prop-2-yn-1-yl)-1,2,4-oxadiazol-5-amine (**3c**).* Yield 68% (123 mg), colorless oil; R_f 0.4 (Hexane-CH_2Cl_2, 1:1). ^{1}H NMR (300 MHz) δ 1.11–1.26, 1.35–1.50, 1.64–1.78, 1.87–1.99 (m, 10H, cyclohexyl), 2.27 (t, 1H, J = 2.3 Hz, CH), 3.98 (dddd, 1H, $J_{ax\text{-}ax}$ = 11.8 Hz and $J_{ax\text{-}eq}$ = 3.5 Hz, N–CH), 4.28 (d, 2H, J = 2.4 Hz, CH_2), 7.31 (dd, 1H, J = 8.2 and 7.7 Hz, $H_{m\text{-}oxadiazole}$), 7.58 (m, 1H, H *p*-oxadiazole), 7.95 (dd, 1H, J = 8.8 and 1.2 Hz, $H_{o\text{-}oxadiazole}$), 8.18 (s, 1H, $H_{o\text{-}oxadiazole}$). ^{13}C NMR (75 MHz): δ 25.3, 25.7 (2C), 30.5 (2C), 34.5, 59.1, 72.0, 79.5, 122.6, 125.8, 129.8, 130.1, 130.3, 133.6, 167.4, 171,0. ESI-HRMS calcd for $C_{17}H_{19}BrN_3O$ $[M+H]^+$: 360.0711; found: 360.0701.

*4.1.2.4. N-Cyclohexyl-3-(3-nitrophenyl)-N-(prop-2-yn-1-yl)-1,2,4-oxadiazol-5-amine (**3d**).* Yield 63% (102 mg), colorless oil, R_f = 0.4 (Hexane-CH_2Cl_2, 1:1). ^{1}H NMR (300 MHz): δ 1.12–1.27, 1.36–1.51, 1.66–1.79, 1.89–2.01 (m, 10H, cyclohexyl), 2.29 (t, 1H, J = 2.4 Hz, CH), 4.00 (dddd, 1H, $J_{ax\text{-}ax}$ = 11.7 Hz and $J_{ax\text{-}eq}$ = 3.5 Hz, *N*–CH), 4.30 (d, 2H, J = 2.9 Hz, CH_2), 7.63 (dd, 1H, J = 8.2 and 7.6 Hz, $H_{m\text{-}oxadiazole}$), 8.30–8.37 (m, 2H, $H_{o\text{-}oxadiazole}$ and $H_{p\text{-}oxadiazole}$), 8.87 (dd, 1H, J = 2.3 and 1.8 Hz, $H_{o\text{-}oxadiazole}$). ^{13}C NMR (75 MHz): δ 25.2, 25.7 (2C), 30.5 (2C), 34.5, 59.2, 72.1, 110.0, 122.4, 125.2, 129.6, 129.7, 132.9, 148.4, 166.8, 171.2. ESI-HRMS calcd for $C_{17}H_{19}N_4O_3$ $[M+H]^+$: 327.1457; found: 327.1450.

*4.1.2.5. 3-(4-Bromophenyl)-N-cyclohexyl-N-(prop-2-yn-1-yl)-1,2,4-oxadiazol-5-amine (**3e**).* Yield 95% (171 mg), colorless solid; mp 72–75 °C, R_f 0.92 (Hexane-CH_2Cl_2, 1:9). ^{1}H NMR (300 MHz): δ 1.12–1.26; 1.35–1.49; 1.65–1.78; 1.87–2.00 (m, 10H, cyclohexyl), 2.27 (t, 1H, J = 2.3 Hz, CH), 3.97 (dddd, 1H, $J_{ax\text{-}ax}$ = 12.3 Hz and $J_{ax\text{-}eq}$ = 3.5 Hz, *N*–CH), 4.28 (d, 2H, J = 2.4 Hz, CH_2), 7.58 (m, 2H, H_{Ar}), 7.90 (m, 2H, H_{Ar}). ^{13}C NMR (75 MHz): δ 25.3, 25.7, 30.5, 34.5, 59.1, 72.0, 79.5, 125.1, 126.8, 128.8, 131.8, 167.8, 171.0. ESI-HRMS calcd for $C_{17}H_{19}BrN_3O$ $[M+H]^+$: 360.0711; found: 360.0708.

*4.1.2.6. 3-(4-Chlorophenyl)-N-cyclohexyl-N-(prop-2-yn-1-yl)-1,2,4-oxadiazol-5-amine (**3f**).* Yield 90% (142 mg), colorless solid, mp 62–64 °C; R_f 0.68 (Hexane-CH_2Cl_2, 2:8). ^{1}H NMR (300 MHz): δ 1.11–1.26; 1.34–1.49; 1.65–1.78; 1.87–2.00 (m, 10H, cyclohexyl), 2.27 (t, 1H, J = 2.4 Hz, CH), 3.97 (dddd, 1H, $J_{ax\text{-}ax}$ = 11.7 Hz and $J_{ax\text{-}eq}$ = 3.5 Hz, *N*–CH), 4.28 (d, 2H, J = 2.4 Hz, CH_2), 7.41 (m, 2H, H_{Ar}), 7.96 (m, 2H, H_{Ar}). ^{13}C NMR (75 MHz): δ 25.3, 25.8, 30.5, 34.5, 59.1, 72.0, 79.6, 128.6, 128.8, 136.7, 167.7, 171.0. ESI-HRMS calcd for $C_{17}H_{19}ClN_3O$ $[M+H]^+$: 316.1217; found: 316.1215.

*4.1.2.7. N-Cyclohexyl-3-(4-fluorophenyl)-N-(prop-2-yn-1-yl)-1,2,4-oxadiazol-5-amine (**3g**).* Yield 83% (124 mg), colorless oil, R_f 0.4 (Hexane-CH_2Cl_2, 1:1). ^{1}H NMR (300 MHz): δ 1.11–1.26; 1.34–1.49; 1.64–1.78; 1.87–2.00 (m, 10H, cyclohexyl), 2.27 (t, 1H, J = 2.3 Hz, CH), 3.97 (dddd, 1H, $J_{ax\text{-}ax}$ = 12.3 Hz and $J_{ax\text{-}eq}$ = 3.5 Hz, *N*–CH), 4.28 (d, 2H, J = 2.4 Hz, CH_2), 7.12 (m, 2H, H_{Ar}), 8.02 (m, 2H, H_{Ar}). ^{13}C NMR (75 MHz): δ 25.3, 25.7, 30.5, 34.5, 59.1, 71.9, 79.6, 115.4–115.7 (d, 2C, $J_{C\text{-}F}$ = 21.9 Hz, C_{o-Ar}), 124.02–124.07 (d, 1C, $J_{C\text{-}F}$ = 3.5 Hz, $C_{p\text{-}Ar}$), 129.3–129.4 (d, 2C, $J_{C\text{-}F}$ = 9.3 Hz, C_{m-Ar}), 165.92–167.95 (d, 1C, $J_{C\text{-}F}$ = 250.9 Hz, $C_{ipso\text{-}Ar}$), 167.6, 170.9. ESI-HRMS calcd for $C_{17}H_{19}FN_3O$ $[M+H]^+$: 300.1512; found: 300.1507.

*4.1.2.8. N-Cyclohexyl-N-(prop-2-yn-1-yl)-3-[4-(trifluoromethyl) phenyl]-1,2,4-oxadiazol-5-amine (**3h**).* Yield 82% (144 mg), colorless solid, mp 53–56 °C; R_f 0.81 (Hexane-CH_2Cl_2, 2:8). ^{1}H NMR (300 MHz): δ 1.12–1.26; 1.35–1.50; 1.63–1.79; 1.88–2.00 (m, 10H, cyclohexyl), 2.28 (t, 1H, J = 2.4 Hz, CH), 3.99 (dddd, 1H, $J_{ax\text{-}ax}$ = 11.7 Hz and $J_{ax\text{-}eq}$ = 3.5 Hz, *N*–CH), 4.30 (d, 2H, J = 2.4 Hz, CH_2), 6.70 (d, 2H, J = 8.2 Hz, H_{Ar}), 8.15 (d, 2H, J = 8.2 Hz, H_{Ar}). ^{13}C NMR (75 MHz): δ 25.3, 25.7, 30.5, 34.6, 59.2, 72.1, 79.4, 125.5, 125.5, 127.6, 129.3, 131.3, 132.1, 132.5, 167.4, 171.1. ESI-HRMS calcd for $C_{18}H_{19}F_3N_3O$ $[M+H]^+$: 350.1480; found: 350.1477.

*4.1.2.9. N-Cyclohexyl-3-(4-nitrophenyl)-N-(prop-2-yn-1-yl)-1,2,4-oxadiazol-5-amine (**3i**).* Yield 93% (152 mg), colorless solid, mp 104–105 °C, R_f = 0.4 (Hexane-CH_2Cl_2, 1:1). ^{1}H NMR (300 MHz): δ 1.13–1.27; 1.35–1.49; 1.66–1.79; 1.88–2.00 (m, 10H, cyclohexyl), 2.29 (t, 1H, J = 2.3 Hz, CH), 3.98 (dddd, 1H, $J_{ax\text{-}ax}$ = 11.7 Hz and $J_{ax\text{-}eq}$ = 3.5 Hz, *N*–CH), 4.30 (d, 2H, J = 2.4 Hz, CH_2), 8.20 (m, 2H, H_{Ar}), 8.29 (m, 2H, H_{Ar}). ^{13}C NMR (75 MHz): δ 25.2, 25.7, 30.5, 34.6, 59.3, 72.2, 79.3, 123.8, 128.2, 133.9, 149.1, 166.9, 171.2. ESI-HRMS calcd for $C_{17}H_{19}N_4O_3$ $[M+H]^+$: 327.1457; found: 327.1451.

*4.1.2.10. N-Cyclohexyl-3-(4-methylphenyl)-N-(prop-2-yn-1-yl)-1,2,4-oxadiazol-5-amine (**3j**).* Yield 86% (127 mg), colorless oil, R_f 0.6 (Hexane-CH_2Cl_2 2:8). ^{1}H NMR (300 MHz): δ 1.11–1.26; 1.34–1.49; 1.64–1.78; 1.87–2.00 (m, 10H, cyclohexyl), 2.26 (t, 1H, J = 2.3 Hz, CH), 2.40 (s, 3H, CH_3), 3.98 (dddd, 1H, $J_{ax\text{-}ax}$ = 11.8 Hz and $J_{ax\text{-}eq}$ = 3.6 Hz, *N*–CH), 4.29 (d, 2H, J = 2,.3 Hz, CH_2), 7.24 (d, 2H, J = 8.2 Hz, H_{Ar}), 7.91 (d, 2H, J = 8.2 Hz, H_{Ar}). ^{13}C NMR (75 MHz): δ 21.5, 25.3, 25.7, 29.7, 30.5, 34.4, 59.0, 71.9, 97.3, 125.0, 127.2, 129.2, 170.8. ESI-HRMS calcd for $C_{18}H_{22}N_3O$ $[M+H]^+$: 296.1763; found: 296.1758.

*4.1.2.11. N-Cyclohexyl-3-(4-methoxyphenyl)-N-(prop-2-yn-1-yl)-1,2,4-oxadiazol-5-amine (**3k**).* Yield 87% (140 mg), colorless solid, mp 88–89 °C; R_f 0.3 (Hexane-CH_2Cl_2, 1:1). ^{1}H (300 MHz): δ 1.12–1.26; 1.34–1.49; 1.64–1.78; 1.87–1.99 (m, 10H, cyclohexyl), 2.26 (t, 3H, J = 2.3 Hz, CH), 3.86 (s, 3H, CH_3), 3.97 (dddd, 1H, $J_{ax\text{-}ax}$ = 11.7 Hz and $J_{ax\text{-}eq}$ = 3.5 Hz, *N*–CH), 4.28 (d, 2H, J = 2.4 Hz, CH_2) 6.96 (m, 2H, H_{Ar}), 7.96 (m, 2H, H_{Ar}). ^{13}C NMR (75 MHz): δ 25.3, 25.8, 30.5, 34.4, 55.3, 59.0, 71.8, 79.8, 113.9, 120.3, 128.8, 161.5, 168.2, 170.7. ESI-HRMS calcd for $C_{18}H_{22}N_3O_2$ $[M+H]^+$: 312.1712; found: 312.1705.

*4.1.2.12. N-cyclohexyl-3-(4-ethynylphenyl)-N-(prop-2-yn-1-yl)-1,2,4-oxadiazol-5-amine (**3l**).* Yield 89% (136 mg), colorless solid, mp 87–89 °C; R_f 0.45 (Hexane-CH_2Cl_2, 1:1). ^{1}H NMR (300 MHz): δ 1.11–1.26; 1.34–1.49; 1.64–1.77; 1.87–1.99 (m, 10H, cyclohexyl), 2.27 (t, 2H, J = 2.4 Hz, CH), 3.18 (dddd, 1H, $J_{ax\text{-}ax}$ = 11.7 Hz and $J_{ax\text{-}eq}$ = 3.5 Hz, *N*–CH), 4.28 (d, 2H, J = 2.4 Hz, CH_2), 7.56 (d, 2H, J = 8.2 Hz, H_{Ar}), 7.99 (d, 2H, J = 8.2 Hz, H_{Ar}). ^{13}C NMR (75 MHz): δ 25.2, 25.7, 30.5, 34.5, 59.1, 72.0, 78.8, 79.5, 83.2, 127.1, 128.1, 132.2, 167.8, 170.9. ESI-HRMS calcd for $C_{19}H_{20}N_3O$ $[M+H]^+$: 306.1606; found: 306.1598.

*4.1.2.13. N-Cyclohexyl-N-(prop-2-yn-1-yl)-3-[4-(prop-2-yn-1-yloxy) phenyl]-1,2,4-oxadiazol-5-amine (**3m**).* Yield 80% (134 mg), colorless solid, mp 82–85 °C; R_f 0.6 (Hexane-CH_2Cl_2, 2:8). ^{1}H NMR (300 MHz): δ 1.12–1.26, 1.35–1.48, 1.64–1.78, 1.87–1.99 (m, 10H, cyclohexyl), 2.26 (t, 1H, J = 2.3 Hz, CH), 2.54 (t, 1H, J = 2.4 Hz, CH), 3.97 (dddd, 1H, $J_{ax\text{-}ax}$ = 11.7 Hz and $J_{ax\text{-}eq}$ = 3.5 Hz, *N*–CH), 4.28 (d, 2H, J = 2.4 Hz, CH_2), 4.74 (d, 2H, J = 2.4 Hz, CH_2), 7.03 (d, 2H, J = 8.8 Hz, H_{Ar}), 7.98 (d, 2H, J = 8.8 Hz, H_{Ar}). ^{13}C NMR (75 MHz): δ 25.3, 25.8 (2C), 30.5 (2C), 34.5, 55.8, 59.0, 71.9, 75.8, 78.1, 79.7, 114.8 (2C), 121.3, 128.8 (3C), 159.4, 168.1. ESI-HRMS calcd for $C_{20}H_{22}N_3O_2$ $[M+H]^+$: 336.1712; found: 336.1704.

*4.1.3. Synthesis of 1,2,4-oxadiazole-1,2,3-triazole-glycerosugars **(5a-k)***

$CuSO_4 \cdot 5H_2O$ (0.09 mmol), sodium ascorbate (0.135 mmol) and alkyne (**3a-k**) (0.3 mmol) were mixed in water (1.5 mL) in a Schlenk flask under argon. This mixture was added into another Schlenk flask containing 0.2 mmol of the azido-carbohydrate **4** (74.2 mg) dissolved in 1.5 mL of dichloromethane. The mixture was stirred at room temperature for 45 min. Then, the solvent was removed, and the residue was purified by column chromatography using hexane-ethyl acetate, 1:1.

*4.1.3.1. N-Cyclohexyl-N-[1-(1′-O-(4,6-di-O-acetyl-2,3-dideoxy-α-D-erythro-hex-2-enopyranosyl)-(2′-acetyl-3′-deoxy-sn-glyceryl-1H-1,2,3-triazol-4-yl)methyl]-3-phenyl-1,2,4-oxadiazol-5-amine (**5a**).* Yield 78% (102 mg), colorless oil, $[\alpha]_D^{25} = +30$ (*c* 0.2, CH_2Cl_2); R_f 0.3 (Hexane-EtOAc, 1:1).

^{1}H NMR (300 MHz): *δ* 1.16–1.44, 1.64–1.95 (m, 10H, cyclohexyl), 1.94 (s, 3H, CH_3), 2.07 (s, 3H, CH_3), 2.08 (s, 3H, CH_3), 3.53 (dd, 1H, J = 10.6 and 4.7 Hz, H-3'a), 3.82 (dd, 1H, J = 10.5 and 5.8 Hz, H-3'b), 3.96–4.02 (m, 1H, N–CH, cyclohexyl), 4.07 (ddd, 1H, J = 9.4, 5.3 and 2.4 Hz, H-5), 4.14 (dd, 1H, J = 12.3 and 2.4 Hz, H-6a), 4.26 (dd, 1H, J = 12.3 and 5.3 Hz, H-6b), 4.58 (dd, 1H, J = 14.1 and 6.5 Hz, H-1'a), 4.64 (dd, 1H, J = 14.0 and 4.1 Hz, H-1'b), 4.78 (s, 2H, CH_2–N), 4.98 (br s, 1H H-1), 5.27–5.31 (m, 2H, H-2′ and H-4), 5.78 (app dt, J = 9.8, 3.0 and 3.0 Hz, H-2), 5.89 (br d, 1H, *J* = 9.7 Hz, H-2), 7.42–7.48 (m, 3H, H_{Ar}), 7.71 (s, 1H, H-5'$_{triaz}$), 8.00–8.03 (m, 2H, H_{Ar}). ^{13}C NMR (75 MHz): *δ* 20.6 ($\underline{C}H_3CO$), 20.7 ($\underline{C}H_3CO$), 20.9 ($\underline{C}H_3CO$), 25.1 (cyclohexyl), 25.7 (2C, cyclohexyl), 30.8 (2C, cyclohexyl), 40.4 (N-$C_{cyclohexyl}$), 50.1 (C-1′), 59.3 (CH_2N-$C_{cyclohexyl}$), 62.8 (C-6), 65.1 (C-4), 66.3 (C-3′), 67.1 (C-5), 70.4 (C-2′), 94.6 (C-1), 124.1 (C5'$_{triaz}$), 126.8 (C-2), 127.1 (2C_{Ar}), 127.8 (C_{Ar}), 128.6 (2C, C_{Ar}), 129.7 (C-3), 130.7 (C_{Ar}), 145.0 (C4'$_{triaz}$), 168.4 (C_{oxad}), 169.6 (C_{oxad}), 170.2 (OAc), 170.7 (OAc), 171.1 (OAc). ESI-HRMS calcd for $C_{32}H_{41}N_6O_9$ $[M+H]^+$: 653.2935; found: 653.2932.

*4.1.3.2. N-Cyclohexyl-N-[1-(1′-O-(4,6-di-O-acetyl-2,3-dideoxy-α-D-erythro-hex-2-enopyranosyl)-(2′-acetyl-3′-deoxy-sn-glyceryl-1H-1,2,3-triazol-4-yl)methyl]-3-(3-methylphenyl)-1,2,4-oxadiazol-5-amine (**5b**).* Yield 64% (85 mg), colorless oil, $[\alpha]_D^{25} = +42$ (*c* 0.2, CH_2Cl_2); R_f 0.5 (Hexane-EtOAc, 1:1). ^{1}H NMR (300 MHz): *δ* 1.15–1.40, 1.66–1.87 (m, 10H, cyclohexyl), 1.94 (s, 3H, CH_3), 2.07 (s, 3H, CH_3), 2.08 (s, 3H, CH_3), 2,41 (s, 3H, CH_3), 3.53 (dd, 1H, J = 10.6 and 4.7 Hz, H-3'a), 3.83 (dd, 1H, J = 10.6 and 5.3 Hz, H-3'b), 3.95–4.01 (m, 1H, N–CH, cyclohexyl), 4.07 (ddd, 1H, J = 9.1, 5.3 and 2.4 Hz, H-5), 4.14 (dd, 1H, J = 12.4 and 2.4 Hz, H-6a), 4.26 (dd, 1H, J = 12.3 and 5.3 Hz, H-6b), 4.57 (dd, 1H, J = 14.4 and 7.1 Hz, H-1'a), 4.64 (dd, 1H, J = 14.3 and 4.7 Hz, H-1'b), 4.77 (s, 2H, CH_2–N), 4.97 (br s, 1H, H-1), 5.27–5.32 (m, 2H, H-4 and H-2′), 5.78 (app dt, 1H, J = 10.2, 2.4 and 2.4 Hz, H-2), 5.89 (br d, 1H, *J* = 10.4 Hz, H-3), 7.30–7.32 (m, 1H, H_{Ar}), 7.33–7.36 (m, 1H, H_{Ar}), 7.70 (s, 1H, H_{triaz}), 7.79–7.82 (m, 2H, H_{Ar}). ^{13}C NMR (75 MHz): *δ* 20.6 ($\underline{C}H_3CO$), 20.7 ($\underline{C}H_3CO$), 20.9 ($\underline{C}H_3CO$), 21.3 (CH_3), 25.1 (cyclohexyl), 25.7 (2C, cyclohexyl), 30.8 (2C, cyclohexyl), 40.4 (N-$C_{cyclohexyl}$), 50.0 (C-1′), 59.2 (CH_2N-$C_{cyclohexyl}$), 62.8 (C-6), 65.1 (C-4), 66.3 (C-3′), 67.1 (C-5), 70.4 (C-2′), 94.6 (C-1), 124.1 (C5'$_{triaz}$), 124.6, 126.8 (C-2), 127.6 (C_{Ar}), 128.5 (C_{Ar}), 129.7 (C-3), 138.3 (C_{Ar}), 145.1 (C4'$_{triaz}$), 168.6 (C_{oxad}), 169.6 (C_{oxad}), 170.1 (OAc), 170.7 (OAc), 171.1 (OAc). ESI-HRMS calcd for $C_{33}H_{43}N_6O_9$ $[M+H]^+$: 667.3091; found: 667.3083.

*4.1.3.3. N-Cyclohexyl-N-[1-(1′-O-(4,6-di-O-acetyl-2,3-dideoxy-α-D-erythro-hex-2-enopyranosyl)-(2′-acetyl-3′-deoxy-sn-glyceryl-1H-1,2,3-triazol-4-yl)methyl]-3-(3-bromophenyl)-1,2,4-oxadiazol-5-amine (**5c**).* Yield 47% (147 mg), colorless oil, $[\alpha]_D^{25} = +10$ (*c* 0.2, CH_2Cl_2); R_f 0.5 (Hexane-EtOAc, 1:1). ^{1}H NMR (300 MHz): *δ* 1.16–1.43, 1.65–1.87 (m, 10H, cyclohexyl), 1.96 (s, 3H, CH_3), 2.08 (s, 3H, CH_3), 2.09 (s, 3H, CH_3), 3.54 (dd, 1H, J = 10.9 and 4.7 Hz, H-3'a), 3.83 (dd, 1H, J = 10.9 and 5.6 Hz, H-3'b), 3.97–4.03 (m, 1H, N–CH, cyclohexyl), 4.08 (ddd, 1H, J = 9.6, 5.2 and 2.3 Hz, H-5), 4.15 (dd, 1H, J = 12.4 and 2.3 Hz, H-6a), 4.26 (dd, 1H, J = 12.4 and 5.2 Hz, H-6b), 4.59 (dd, 1H, J = 14.3 and 6.4 Hz, H-1'a), 4.64 (dd, 1H, J = 14.4 and 4.4 Hz, H-1'b), 4.77 (s, 2H, CH_2–N), 4.99 (br s, 1H, H-1), 5.28–5.32 (m, 2H, H-2′ and H-4), 5.78 (ddd, 1H, J = 10.0, 2.6 and 2.1 Hz, H-2), 5.90 (d, 1H, *J* = 10.3 Hz, H-3), 7.32 (dd, 1H, J = 8.0 and 7.9 Hz, H_{Ar}), 7.60 (ddd, 1H, J = 11.2, 2.0 and 0.8 Hz, H_{Ar}), 7.68 (s, 1H, H $_{triaz}$), 7.94 (app dt, 1H, J = 7.9, 1.2 and 1.2 Hz, H_{Ar}), 8.16 (dd, 1H, J = 2.0 and 1.5 Hz, H_{Ar}). ^{13}C NMR (75 MHz): *δ* 20.6 ($\underline{C}H_3CO$), 20.7 ($\underline{C}H_3CO$), 20.9 ($\underline{C}H_3CO$), 25.1 (cyclohexyl), 25.7 (2C, cyclohexyl), 30.8 (2C, cyclohexyl), 40.4 (N-$C_{cyclohexyl}$), 50.1 (C-1′), 59.4 (CH_2N-$C_{cyclohexyl}$), 62.8 (C-6), 65.1 (C-4), 66.3 (C-3′), 67.1 (C-5), 70.4 (C-2′), 94.6 (C-1), 122.6 (C5'$_{triaz}$), 124.0, 125.6, 126.8 (C-2), 129.7 (C_{Ar}), 129.8 (C-3), 130.2 (2C_{Ar}), 133.7 (C_{Ar}), 144.9 (C4'$_{triaz}$), 167.3 (C_{oxad}), 169.6 (C_{oxad}), 170.2 (OAc), 170.7 (OAc), 171.2 (OAc). ESI-HRMS calcd for $C_{32}H_{40}BrN_6O_9$ $[M+H]^+$: 731.2040; found: 731.2033.

*4.1.3.4. N-Cyclohexyl-N-[1-(1′-O-(4,6-di-O-acetyl-2,3-dideoxy-α-D-erythro-hex-2-enopyranosyl)-(2′-acetyl-3′-deoxy-sn-glyceryl-1H-1,2,3-triazol-4-yl)methyl]-3-(3-nitrophenyl)-1,2,4-oxadiazol-5-amine (**5d**).* Yield 57% (79 mg), colorless oil, $[\alpha]_D^{25} = +7.5$ (*c* 0.2, CH_2Cl_2); R_f 0.5 (Hexane-EtOAc, 1:1).

^{1}H NMR (300 MHz): *δ* 1.17–1.46, 1.66–1.89 (m, 10H, cyclohexyl), 1.98 (s, 3H, CH_3), 2.07 (s, 3H, CH_3), 2.09 (s, 3H, CH_3), 3.56 (dd, 1H, J = 11.2 and 4.7 Hz, H-3'a), 3.85 (dd, 1H, J = 11.2 and 5.9 Hz, H-3'b), 3.99–4.03 (m, 1H, CH–N), 4.07 (ddd, 1H, J = 12.3, 5.3 and 2.9 Hz, H-5), 4.15 (dd, 1H, J = 12.3 and 2.9 Hz, H-6a), 4.25 (dd, 1H, J = 12.4 and 5.3 Hz, H-6b), 4.59 (dd, 1H, J = 14.7 and 7.1 Hz, H-1'a), 4.65 (dd, 1H, J = 14.7 and 4.7 Hz, H-1'b), 4.79 (s, 2H, CH_2–N), 4.99 (br s, 1H, H-1), 5.27–5.32 (m, 2H, H-2′ and H-4), 5.79 (app dt, 1H, J = 10.0, 2.3 and 2.3 Hz, H-2), 5.90 (br d, 1H, *J* = 9.9 Hz, H-3), 7.65 (dd, 1H, J = 7.9 and 8.2 Hz, H_{Ar}), 7.69 (s, 1H, H_{triaz}), 8.31–8.36 (m, 2H, H_{Ar}), 8.85–8.86 (m, 1H, H_{Ar}). ^{13}C NMR (75 MHz): *δ* 20.6 ($\underline{C}H_3CO$), 20.7 ($\underline{C}H_3CO$), 20.9 ($\underline{C}H_3CO$), 25.1 (cyclohexyl), 25.7 (2C, cyclohexyl), 30.8 (2C, cyclohexyl), 40.5 (N-$C_{cyclohexyl}$), 50.1 (C-1′), 59.6 (CH_2N-$C_{cyclohexyl}$), 62.8 (C-6), 65.1 (C-4), 66.4 (C-3′), 67.2 (C-5), 70.4 (C-2′), 94.6 (C-1), 122.3 (C5'$_{triaz}$), 123.9, 125.2, 126.8 (C-2), 129.7 (C_{Ar}), 129.8 (C-3), 132.8 (C_{Ar}), 144.6 (C_{Ar}), 148.5 (C4'$_{triaz}$), 166.8 (C_{oxad}), 169.6 (C_{oxad}), 170.2 (OAc), 170.7 (OAc), 171.4 (OAc). ESI-HRMS calcd for $C_{32}H_{40}N_7O_{11}$ $[M+H]^+$: 698.2786; found: 698.2783.

*4.1.3.5. N-Cyclohexyl-N-[1-(1′-O-(4,6-di-O-acetyl-2,3-dideoxy-α-D-erythro-hex-2-enopyranosyl)-(2′-acetyl-3′-deoxy-sn-glyceryl-1H-1,2,3-triazol-4-yl)methyl]-3-(4-bromophenyl)-1,2,4-oxadiazol-5-amine (**5e**).* Yield 90% (132 mg), colorless solid, mp 72–75 °C, $[\alpha]_D^{25} = +25$ (*c* 0.1, CH_2Cl_2); R_f 0.4 (Hexane-EtOAc, 1:1). ^{1}H NMR (300 MHz): *δ* 1.15–1.43, 1.66–1.87 (m, 10H, cyclohexyl), 1.95 (s, 3H, CH_3), 2.08 (s, 3H, CH_3), 2.09 (s, 3H, CH_3), 3.54 (dd, 1H, J = 10.6 and 4.7 Hz, H-3'a), 3.83 (dd, 1H, J = 10.5 and 5.3 Hz, H-3'b), 3.91–4.03 (m, 1H, N–CH, cyclohexyl), 4.08 (ddd, 1H, J = 9.4, 5.3 and 2.3 Hz, H-5), 4.15 (dd, 1H, J = 12.4 and 2.4 Hz, H-6a), 4.26 (dd, 1H, J = 12.3 and 5.3 Hz, H-6b), 4.57 (dd, 1H, J = 14.1 and 6.4 Hz, H-1'a), 4.64 (dd, 1H, J = 14.1 and 4.1 Hz, H-1'b), 4.76 (s, 2H, CH_2–N), 4.98 (br s, 1H, H-1), 5.25–5.32 (m, 2H, H-4 and H-2′), 5.78 (app dt, 1H, J = 9.9, 2.3 and 2.3 Hz, H-2), 5.90 (d, 1H, *J* = 10.0 Hz, H-3), 7.54–7.60 (m, 2H, H_{Ar}), 7.76 (s, 1H, H_{triaz}), 7.87–7.91 (m, 2H, H_{Ar}). ^{13}C NMR (75 MHz): *δ* 20.6 ($\underline{C}H_3CO$), 20.7 ($\underline{C}H_3CO$), 20.9 ($\underline{C}H_3CO$), 25.1 (cyclohexyl), 25.7 (2C, cyclohexyl), 30.8 (2C, cyclohexyl), 40.4 (N-$C_{cyclohexyl}$), 50.0 (C-1′), 59.4 (CH_2N-$C_{cyclohexyl}$), 62.8 (C-6), 65.1 (C-4), 66.3 (C-3′), 67.1 (C-5), 70.4 (C-2′), 94.6 (C-1), 124.0 (C5'$_{triaz}$), 125.2, 126.8 (C-2), 128.7 (2C_{Ar}), 129.8 (C-3), 131.8 (C_{Ar}), 144.9 (C4'$_{triaz}$), 167.7 (C_{oxad}), 169.6 (C_{oxad}), 170.2 (OAc), 170.7 (OAc), 171.2 (OAc). ESI-HRMS calcd for $C_{32}H_{40}BrN_6O_9$ $[M+H]^+$: 731.2040; found: 731.2037.

*4.1.3.6. N-Cyclohexyl-N-[1-(1′-O-(4,6-di-O-acetyl-2,3-dideoxy-α-D-erythro-hex-2-enopyranosyl)-(2′-acetyl-3′-deoxy-sn-glyceryl-1H-1,2,3-triazol-4-yl)methyl]-3-(4-chlorophenyl)-1,2,4-oxadiazol-5-amine (**5f**).* Yield 89% (122 mg), colorless oil, $[\alpha]_D^{25} = +10$ (*c* 0.1, CH_2Cl_2); R_f 0.4 (Hexane-EtOAc, 1:1). ^{1}H NMR (300 MHz): δ 1.16–1.44, 1.67–1.87 (m, 10H, cyclohexyl), 1.95 (s, 3H, CH_3), 2.08 (s, 3H, CH_3), 2.09 (s, 3H, CH_3), 3.54 (dd, 1H, J = 11.2 and 4.7 Hz, H-3'a), 3.83 (dd, 1H, J = 11.1 and 5.3 Hz, H-3'b), 3.96–4.03 (m, 1H, N–CH, cyclohexyl), 4.07 (ddd, 1H, J = 9.4, 5.3 and 1.7 Hz, H-5), 4.15 (dd, 1H, J = 12.3 and 1.8 Hz, H-6a), 4.26 (dd, 1H, J = 12.3 and 5.3 Hz, H-6b), 4.58 (dd, 1H, J = 14.3 and 6.4 Hz, H-1'a), 4.64 (dd, 1H, J = 14.5 and 4.7 Hz, H-1'b), 4.77 (s, 2H, CH_2–N), 4.99 (br s, 1H, H-1), 5.26–5.32 (m, 2H, H-4 and H-2′), 5.79 (app dt, 1H, J = 10.6, 1.7 and 1.7 Hz, H-2), 5.90 (br d, 1H, *J* = 10.6 Hz, H-3), 7.42 (d, 2H, *J* = 8.8 Hz, H_{Ar}), 7.69 (s, 1H, H_{triaz}), 7.95 (d, 2H, *J* = 8.8 Hz, H_{Ar}). ^{13}C NMR (75 MHz): δ 20.6 ($\underline{C}H_3CO$), 20.7 ($\underline{C}H_3CO$), 20.9 ($\underline{C}H_3CO$), 25.1 (cyclohexyl), 25.7 (2C, cyclohexyl), 30.8 (2C, cyclohexyl), 40.4 (N-$C_{cyclohexyl}$), 50.1 (C-1′), 59.4 (CH_2N-$C_{cyclohexyl}$), 62.8 (C-6), 65.1 (C-4), 66.3 (C-3′), 67.2 (C-5), 70.4 (C-2′), 94.6 (C-1), 124.0 (C5'$_{triaz}$), 126.3, 126.8 (C-2), 128.5 (2C_{Ar}), 128.9, 129.8 (C-3), 136.8 (C_{Ar}), 144.9 (C4'$_{triaz}$), 167.6 (C_{oxad}), 169.6 (C_{oxad}), 170.2 (OAc), 170.7 (OAc), 171.2 (OAc). ESI-HRMS calcd for $C_{32}H_{40}ClN_6O_9$ $[M+H]^+$: 687.2545; found: 687.2539.

*4.1.3.7. N-Cyclohexyl-N-[1-(1′-O-(4,6-di-O-acetyl-2,3-dideoxy-α-D-erythro-hex-2-enopyranosyl)-(2′-acetyl-3′-deoxy-sn-glyceryl-1H-1,2,3-triazol-4-yl)methyl]-3-(4-fluorophenyl)-1,2,4-oxadiazol-5-amine (**5g**).* Yield 85% (114 mg), colorless oil, $[\alpha]_D^{25} = +22.5$ (*c* 0.2, CH_2Cl_2); R_f 0.4 (Hexane- EtOAc, 1:1). ^{1}H NMR (300 MHz): δ 1.16–1.39, 1.67–1.87 (m, 10H, cyclohexyl), 1.95 (s, 3H, CH_3), 2.08 (s, 3H, CH_3), 2.09 (s, 3H, CH_3), 3.54 (dd, 1H, J = 11.0 and 4.7 Hz, H-3'a), 3.83 (dd, 1H, J = 10.8 and 5.3 Hz, H-3'b), 3.94–4.03 (m, 1H, N–CH, cyclohexyl), 4.07 (ddd, 1H, J = 9.9, 5.3 and 2.3 Hz, H-5), 4.15 (dd, 1H, J = 12.3 and 2.9 Hz, H-6a), 4.26 (dd, 1H, J = 12.3 and 5.3 Hz, H-6b), 4.58 (dd, 1H, J = 14.1 and 6.4 Hz, H-1'a), 4.64 (dd, 1H, J = 14.1 and 4.7 Hz, H-1'b), 4.77 (s, 2H, CH_2–N), 4.99 (br s, 1H, H-1), 5.26–5.32 (m, 2H, H-4 and H-2′), 5.79 (app dt, 1H, J = 10.0, 2.3 and 2.3 Hz, H-2), 5.90 (d, 1H, *J* = 10.3 Hz, H-3), 7.11–7.16 (m, 2H, H_{Ar}), 7.68 (s, 1H, H_{triaz}), 7.99–8.04 (m, 2H, H_{Ar}). ^{13}C NMR (75 MHz): δ 20.6 ($\underline{C}H_3CO$), 20.7 ($\underline{C}H_3CO$), 20.9 ($\underline{C}H_3CO$), 25.1 (cyclohexyl), 25.7 (2C, cyclohexyl), 30.8 (2C, cyclohexyl), 40.4 (N-$C_{cyclohexyl}$), 50.0 (C-1′), 59.4 (CH_2N-$C_{cyclohexyl}$), 62.8 (C-6), 65.1 (C-4), 66.3 (C-3′), 67.2 (C-5), 70.4 (C-2′), 94.6 (C-1), 115.6–115.9 (d, 2C, $J_{C\text{-}F}$ = 22.0 Hz, C_{o-Ar}), 123.9 (C5'$_{triaz}$), 124.0 (d, 1C, $J_{C\text{-}F}$ = 6.8 Hz, $C_{p\text{-}Ar}$), 126.8 (C-2), 129.2–129.3 (d, 2C, $J_{C\text{-}F}$ = 8.1 Hz, C_{m-Ar}), 129.8 (C-3), 145.0 (C4'$_{triaz}$), 162.7–166.0 (d, 1C, $J_{C\text{-}F}$ = 250.8 Hz, $C_{ipso\text{-}Ar}$), 167.6 (C_{oxad}), 169.6 (C_{oxad}), 170.2 (OAc), 170.7 (OAc), 171.2 (OAc). ESI-HRMS calcd for $C_{32}H_{40}FN_6O_9$ $[M+H]^+$: 671.2841; found: 671.2835.

*4.1.3.8. N-Cyclohexyl-N-[1-(1′-O-(4,6-di-O-acetyl-2,3-dideoxy-α-D-erythro-hex-2-enopyranosyl)-(2′-acetyl-3′-deoxy-sn-glyceryl-1H-1,2,3-triazol-4-yl)methyl]-3-(4-trifluoromethylphenyl)-1,2,4-oxadiazol-5-amine (**5h**).* Yield 87% (125 mg), colorless oil, $[\alpha]_D^{25} = +35$ (*c* 0.1, CH_2Cl_2); R_f 0.5 (Hexane-EtOAc, 1:1).

^{1}H NMR (300 MHz): δ 1.15–1.44, 1.65–1.88 (m, 10H, cyclohexyl), 1.95 (s, 3H, CH_3), 2.07 (s, 3H, CH_3), 2.08 (s, 3H, CH_3), 3.55 (dd, 1H, J = 10.6 and 4.7 Hz, H-3'a), 3.84 (dd, 1H, J = 10.5 and 5.3 Hz, H-3'b), 3.96–4.03 (m, 1H, N–CH, cyclohexyl), 4.07 (ddd, 1H, J = 9.9, 5.2 and 2.7 Hz, H-5), 4.15 (dd, 1H, J = 12.0 and 2.6 Hz, H-6a), 4.25 (dd, 1H, J = 12.2 and 5.3 Hz, H-6b), 4.58 (dd, 1H, J = 14.4 and 6.4 Hz, H-1'a), 4.64 (dd, 1H, J = 14.4 e 4.7 Hz, H-1'b), 4.78 (s, 2H, CH_2–N), 4.98 (br s, 1H, H-1), 5.26–5.31 (m, 2H, H-4 and H-2′), 5.78 (app dt, 1H, J = 10.4, 3.0 and 3.0 Hz, H-2), 5.90 (d, 1H, *J* = 10.2 Hz, H-3), 7.68 (s, 1H, H_{triaz}), 7.71 (d, 2H, *J* = 8.2 Hz, H_{Ar}), 8.14 (d, 2H, *J* = 8.2 Hz, H_{Ar}). ^{13}C NMR (75 MHz): δ 20.6 ($\underline{C}H_3CO$), 20.7 ($\underline{C}H_3CO$), 20.9 ($\underline{C}H_3CO$), 25.1 (cyclohexyl), 25.7 (2C, cyclohexyl), 30.8 (2C, cyclohexyl), 40.5 (N-$C_{cyclohexyl}$), 50.0 (C-1′), 59.5 (CH_2N-$C_{cyclohexyl}$), 62.8 (C-6), 65.1 (C-4), 66.4 (C-3′), 67.1 (C-5), 70.4 (C-2′), 94.6 (C-1), 122.0 (C5'$_{triaz}$), 123.9, 125.5 (q, 1C, $J_{C\text{-}F}$ = 4.6 Hz, $\underline{C}F_3$), 126.8 (C-2), 127.5 (2C_{Ar}), 129.8 (C-3), 131.3, 132.7, 144.8 (C4'$_{triaz}$), 167.4 (C_{oxad}), 169.6 (C_{oxad}), 170.1 (OAc), 170.7 (OAc), 171.3 (OAc). ESI-HRMS calcd for $C_{33}H_{40}F_3N_6O_9$ $[M+H]^+$: 721.2809; found: 721.2799.

*4.1.3.9. N-Cyclohexyl-N-[1-(1′-O-(4,6-di-O-acetyl-2,3-dideoxy-α-D-erythro-hex-2-enopyranosyl)-(2′-acetyl-3′-deoxy-sn-glyceryl-1H-1,2,3-triazol-4-yl)methyl]-3-(4-nitrophenyl)-1,2,4-oxadiazol-5-amine (**5i**).* Yield 90% (125 mg), colorless oil, $[\alpha]_D^{25} = +10$ (*c* 0.1, CH_2Cl_2); R_f 0.3 (Hexane-EtOAc, 1:1). ^{1}H NMR (300 MHz): δ 1.15–1.45, 1.66–1.88 (m, 10H, cyclohexyl), 1.97 (s, 3H, CH_3), 2.07 (s, 3H, CH_3), 2.08 (s, 3H, CH_3), 3.56 (dd, 1H, J = 10.9 and 4.7 Hz, H-3'a), 3.84 (dd, 1H, J = 11.0 and 5.3 Hz, H-3'b), 3.97–4.03 (m, 1H, N–CH, cyclohexyl), 4.07 (ddd, 1H, J = 11.7, 5.1 and 2.3 Hz, H-5), 4.15 (dd, 1H, J = 12.1 and 2.3 Hz, H-6a), 4.25 (dd, 1H, J = 12.0 and 5.3 Hz, H-6b), 4.58 (dd, 1H, J = 14.4 and 7.0 Hz, H-1'a), 4.65 (dd, 1H, J = 14.3 and 4.1 Hz, H-1'b), 4.78 (s, 2H, CH_2–N), 4.99 (br s, 1H, H-1), 5.26–5.33 (m, 2H, H-4 and H-2′), 5.79 (app dt, 1H, J = 10.0, 2.3 and 2.3 Hz, H-2), 5.90 (d, 1H, *J* = 10.0 Hz, H-3), 7.68 (s, 1H, H_{triaz}), 8.17–8.21 (m, 2H, H_{Ar}), 8.29–8.32 (m, 2H, H_{Ar}). ^{13}C NMR (75 MHz): δ 20.6 ($\underline{C}H_3CO$), 20.7 ($\underline{C}H_3CO$), 20.9 ($\underline{C}H_3CO$), 25.1 (cyclohexyl), 25.7 (2C, cyclohexyl), 30.7 (2C, cyclohexyl), 40.5 (N-$C_{cyclohexyl}$), 50.1 (C-1′), 59.6 (CH_2N-$C_{cyclohexyl}$), 62.7 (C-6), 65.1 (C-4), 66.4 (C-3′), 67.1 (C-5), 70.4 (C-2′), 94.6 (C-1), 123.8 (2C_{Ar}, C5'$_{triaz}$), 126.8 (C-2), 128.1 (2C_{Ar}), 129.8 (C-3), 133.8 (C_{Ar}), 144.8 (C4'$_{triaz}$), 149.2(C_{Ar}), 166.8 (C_{oxad}), 169.6 (C_{oxad}), 170.1 (OAc), 170.7 (OAc), 171.4 (OAc). ESI-HRMS calcd for $C_{32}H_{40}N_7O_{11}$ $[M+H]^+$: 698.2786; found: 698.2781.

*4.1.3.10. N-Cyclohexyl-N-[1-(1′-O-(4,6-di-O-acetyl-2,3-dideoxy-α-D-erythro-hex-2-enopyranosyl)-(2′-acetyl-3′-deoxy-sn-glyceryl-1H-1,2,3-triazol-4-yl)methyl]-3-(4-methylphenyl)-1,2,4-oxadiazol-5-amine (**5j**).* Yield 89% (118 mg), colorless oil, $[\alpha]_D^{25} = +40$ (*c* 0.2, CH_2Cl_2); R_f 0.4 (Hexane-EtOAc, 1:1). ^{1}H NMR (300 MHz): δ 0.39–0.99, 1.22–1.46 (m, 10H, cyclohexyl), 1.50 (s, 3H, CH_3), 1.64 (s, 3H, CH_3), 1.65 (s, 3H, CH_3), 1.97 (s, 3H, CH_3), 3.09 (dd, 1H, J = 10.5 and 4.6 Hz, H-3'a), 3.39 ((dd, 1H, J = 10.6 and 5.3 Hz, H-3'b), 3.51–3.60 (m, 1H, CH–N), 3.64 (ddd, 1H, J = 9.2, 5.3 and 2.0 Hz, H-5), 3.72 (dd, 1H, J = 11.9 and 2.0 Hz, H-6a), 3.82 (dd, 1H, J = 11.9 and 5.3 Hz, H-6'b), 4.13 (dd, 1H, J = 14.5 and 6.6 Hz, H-1'a), 4.20 (dd, 1H, J = 14.5 and 4.6 Hz, H-1'b), 4.33 (s, 2H, CH_2), 4.54 (br s, 1H, H-1), 4.78–4.86 (m, 2H, H-4 and H-2′), 5.34 (app dt, 1H, J = 9.8, 2.0 and 2.0 Hz, H-2), 5.46 (d, 1H, *J* = 10.5 Hz, H-3), 6.80–6.83 (m, 3H, 2H_{Ar} and H_{triaz}), 7.45–7.47 (m, 2H, H_{Ar}). For aromatic part in DMSO-d_6: δ 7.31 (d, 2H, *J* = 7.90 Hz, H_{Ar}), 7.80 (d, 2H, *J* = 7.90 Hz, H_{Ar}), 8.08 (s, 1H, H_{triaz}). ^{13}C NMR (75 MHz in $CDCl_3$): δ 20.6 ($\underline{C}H_3CO$), 20.7 ($\underline{C}H_3CO$), 20.9 ($\underline{C}H_3CO$), 25.1 (cyclohexyl), 25.7 (2C, cyclohexyl), 30.8 (2C, cyclohexyl), 40.4 (N-$C_{cyclohexyl}$), 50.0 (C-1′), 59.2 (CH_2N-$C_{cyclohexyl}$), 62.8 (C-6), 65.1 (C-4), 66.3 (C-3′), 67.1 (C-5), 70.4 (C-2′), 94.6 (C-1), 124.1 (C5'$_{triaz}$), 125.0, 126.7 (C-2), 127.1 (2C_{Ar}), 129.3 (2C_{Ar}), 129.7 (C-3), 141.0 (C_{Ar}), 145.1 (C4'$_{triaz}$), 168.4 (C_{oxad}), 169.6 (C_{oxad}), 170.2 (OAc), 170.7 (OAc), 171.0 (OAc). ESI-HRMS calcd for $C_{33}H_{43}N_6O_9$ $[M+H]^+$: 667.3091; found: 667.3088.

*4.1.3.11. N-Cyclohexyl-N-[1-(1′-O-(4,6-di-O-acetyl-2,3-dideoxy-α-D-erythro-hex-2-enopyranosyl)-(2′-acetyl-3′-deoxy-sn-glyceryl-1H-1,2,3-triazol-4-yl)methyl]-3-(4-methoxyphenyl)-1,2,4-oxadiazol-5-amine (**5k**).* Yield 85% (116 mg), colorless oil, $[\alpha]_D^{25} = +35$ (*c* 0.1, CH_2Cl_2); R_f 0.3 (Hexane-EtOAc, 1:1). ^{1}H NMR (300 MHz): δ 1.11–1.43, 1.66–1.87 (m, 10H, cyclohexyl), 1.95 (s, 3H, CH_3), 2.08 (s, 3H, CH_3), 2.09 (s, 3H, CH_3), 3.53 (dd, 1H, J = 10.5 and 4.7 Hz, H-3'a), 3.83 (dd, 1H, J = 10.6 and 5.3 Hz, H-3'b), 3.86 (s, 3H, OCH_3), 3.95–4.03 (m, 1H, CH cyclohexyl), 4.07 (ddd, 1H, J = 9.4, 5.3 and

2.4 Hz, H-5), 4.15 (dd, 1H, J = 12.3 and 2.9 Hz, H-6a), 4.26 (dd, 1H, J = 12.4 and 5.9 Hz, H-6b), 4.58 (dd, 1H, J = 14.7 and 7.0 Hz, H-1'a), 4.64 (dd, 1H, J = 14.7 and 4.7 Hz, H-1'b), 4.76 (s, 2H, CH_2–N), 4.98 (br s, 1H, H-1), 5.28–5.31 (m, 2H, H-4 and H-2′), 5.78 (app dt, 1H, J = 10.0, 2.3 and 2.3 Hz, H-3), 5.89 (d, 1H, *J* = 10.5 Hz, H-2), 6.95 (d, 2H, *J* = 8.8 Hz, H_{Ar}), 7.72 (s, 1H, H_{triaz}), 7.95 (d, 2H, *J* = 8.9 Hz, H_{Ar}). ^{13}C NMR (75 MHz): δ 20.6 ($\underline{C}H_3CO$), 20.7 ($\underline{C}H_3CO$), 20.9 ($\underline{C}H_3CO$), 25.1 (cyclohexyl), 25.7 (2C, cyclohexyl), 30.8 (2C, cyclohexyl), 40.4 (N-$C_{cyclohexyl}$), 50.0 (C-1′), 55.3 ($O\underline{C}H_3$), 59.2 (CH_2N-$C_{cyclohexyl}$), 62.8 (C-6), 65.1 (C-4), 66.3 (C-3′), 67.1 (C-5), 70.4 (C-2′), 94.6 (C-1), 114.0 ($2C_{Ar}$), 120.2 (C5'$_{triaz}$), 126.8 (C-2), 128.7 ($2C_{Ar}$), 129.7 (C-3), 161.6 (C4'$_{triaz}$), 168.2 (C_{oxad}), 169.6 (C_{oxad}), 170.2 (OAc), 170.7 (OAc), 171.0 (OAc). ESI-HRMS calcd for $C_{33}H_{43}N_6O_{10}$ $[M+H]^+$: 683.3041; found: 683.3035.

*4.1.3.12. N-Cyclohexyl-3-[4–1′-O-(4,6-di-O-acetyl-2,3-dideoxy-α-D-erythro-hex-2-enopyranosyl)-(2′-acetyl-3′-deoxy-sn-glyceryl-1H-1,2,3-triazol-4-yl)phenyl]-1,2,4-oxadiazol-5-amine (**6**).* Yield 91% (110 mg), colorless solid, mp 135–138 °C, $[\alpha]_D^{25}$ = + 9.5 (*c* 0.1, CH_2Cl_2); R_f 0.2 (Hexane-EtOAc, 1:1). ^{1}H NMR (300 MHz): δ 1.18–1.51, 1.63–1.82 (m, 10H, cyclohexyl), 2.07 (s, 3H, CH_3), 2.10 (s, 6H, $2CH_3$), 3.64 (dd, 1H, J = 10.6 and 4.7 Hz, H-3'a), 3.70–3.76 (m, 1H, N–CH cyclohexyl), 3.89 (dd, 1H, J = 10.6 and 5.9 Hz, H-3'b), 4.11 (ddd, 1H, J = 9.4, 5.3 and 2.4 Hz, H-5), 4.19 (dd, 1H, J = 12.3 and 2.4 Hz, H-6a), 4.27 (dd, 1H, J = 12.3 and 5.3 Hz, H-6b), 4.69 (dd, 1H, J = 14.1 and 8.9 Hz, H-1'a), 4.75 (dd, 1H, J = 14.1 and 4.7 Hz, H-1'b), 5.04 (br s, 1H, H-1), 5.24 (d, 1H, *J* = 8.2 Hz, N–H), 5.30–5.42 (m, 2H, H-4 and H-2′), 5.84 (app dt, 1H, J = 10.6, 2.4 and 2.4 Hz, H-2), 5.94 (d, 1H, *J* = 10.6 Hz, H-3), 7.89 (s, 1H, H_{triaz}), 7.91 (d, 2H, *J* = 8.2 Hz, H_{Ar}), 8.30 (d, 2H, *J* = 8.2 Hz, H_{Ar}). ^{13}C NMR (75 MHz): δ 20.7 ($\underline{C}H_3CO$), 20.8 ($\underline{C}H_3CO$), 20.9 ($\underline{C}H_3CO$), 24.6 (2C, cyclohexyl), 25.3 (cyclohexyl), 33.2 (2C, cyclohexyl), 50.1 (C-1′), 52.9 (N-$C_{cyclohexyl}$), 62.8 (C-6), 65.1 (C-4), 66.4 (C-3′), 67.2 (C-5), 70.5 (C-2′), 94.7 (C-1), 120.8 (C5'$_{triaz}$), 125.8 ($2C_{Ar}$), 126.9 (C-2), 127.5, 127.7 ($2C_{Ar}$), 129.8 (C-3), 132.5, 147.5 (C4'$_{triaz}$), 168.0 (C_{oxad}), 169.8 (C_{oxad}), 170.2 (OAc), 170.6 (OAc), 170.7 (OAc). ESI-HRMS calcd for $C_{31}H_{39}N_6O_9$ $[M+H]^+$: 639.2778; found: 639.2774.

*4.1.3.13. N-Cyclohexyl-3-[4–1′-O-(4,6-di-O-acetyl-2,3-dideoxy-α-D-erythro-hex-2-enopyranosyl)-(2′-acetyl-3′-deoxy-sn-glyceryl-1H-1,2,3-triazol-4-ylmethoxy)phenyl]-1,2,4-oxadiazol-5-amine (**7**).* Yield 94% (126 mg), colorless oil, $[\alpha]_D^{25}$ = + 35 (*c* 0.1, CH_2Cl_2); R_f = 0.3 (Hexane-EtOAc, 1:1). ^{1}H NMR (300 MHz): δ 1.18–1.48, 1.63–1.80 (m, 10H, cyclohexyl), 2.03 (s, 3H, CH_3), 2.09 (s, 3H, CH_3), 2.10 (s, 3H, CH_3), 3.58 (dd, 1H, J = 10.8 and 4.9 Hz, H-3'a), 3.63–3.72 (m, 1H, CH–N), 3.84 (dd, 1H, J = 10.9 and 5.9 Hz, H-3'b), 4.09 (ddd, 1H, J = 9.4, 5.0 and 2.4 Hz, H-5), 4.18 (dd, 1H, J = 12.0 and 2.7 Hz, H-6a), 4.27 (dd, 1H, J = 12.1 and 5.3 Hz, H-6b), 4.64 (dd, 1H, J = 14.4 and 6.2 Hz, H-1'a), 4.68 (dd, 1H, J = 14.4 and 4.7 Hz, H-1'b), 5.00 (br s, 1H, H-1), 5.18 (d, 1H, *J* = 8.3 Hz, N–H), 5.28 (s, 2H, CH_2O), 5.30–5.35 (m, 2H, H-2′ and H-4), 5.81 (app dt, 1H, J = 10.3, 2.6 and 2.6 Hz, H-2), 5.92 (d, 1H, *J* = 10.3 Hz, H-3), 7.01–7.04 (m, 2H, H_{Ar}), 7.65 (s, 1H, H_{triaz}), 7.91–7.94 (m, 2H, H_{Ar}). ^{13}C NMR (75 MHz): δ 20.8 (2x$\underline{C}H_3CO$), 20.9 ($\underline{C}H_3CO$), 24.6 (2C, cyclohexyl), 25.3 (cyclohexyl), 33.2 (2C, cyclohexyl), 50.1 (C-1′), 52.8 (N-$C_{cyclohexyl}$), 62.0 (CH_2OAr), 62.8 (C-6), 65.1 (C-4), 66.3 (C-3′), 67.2 (C-5), 70.4 (C-2′), 94.6 (C-1), 114.8 ($2C_{Ar}$), 120.9 (C5'$_{triaz}$), 123.6 ($2C_{Ar}$), 126.9 (C-2), 128.8 ($2C_{Ar}$), 129.8 (C-3), 144.1 (C_{Ar}), 160.0 (C4'$_{triaz}$), 168.0 (C_{oxad}), 169.8 (C_{oxad}), 170.2 (OAc), 170.4 (OAc), 170.7 (OAc). ESI-HRMS calcd for $C_{32}H_{41}N_6O_{10}$ $[M+H]^+$: 669.2884; found: 669.2877.

*4.1.3.14. 1′-O-(4,6-di-O-acetyl-2,3-dideoxy-α-D-erythro-hex-2-enopyranosyl)-(2′-acetyl-3′-deoxy-[4-(5-methyl-3-[4-(methyloxy) phenyl]-1,2,4- oxadiazolyl)]-1H-1,2,3-triazol-1-yl-sn-glycerol (**8**).* 197 mg (0.53 mmol) of azido-sugar **4** and 170 mg (0.79 mmol) of alkyne-oxadiazole **2n** were used.

Yield 64% (198 mg), colorless oil, $[\alpha]_D^{25}$ = + 45 (*c* 0.1, CH_2Cl_2), R_f 0.3 (Hexane-EtOAc, 1:1). ^{1}H NMR (400 MHz): δ 2.03 (s, 3H, CH_3), 2.08 (s, 3H, CH_3), 2.10 (s, 3H, CH_3), 2.63 (s, 3H, CH_3-oxadiazole), 3.58 (dd, 1H, J = 11.0 and 5.9 Hz, H-1'a), 3.84 (dd, 1H, J = 11.0 and 5.9 Hz, H-1'b), 4.09 (ddd, 1H, J = 9.8, 5.1 and 2.3 Hz, H-5), 4.18 (dd, 1H, J = 12.1 and 2.3 Hz, H-6a), 4.27 (dd, 1H, J = 12.1 and 5.1 Hz, H-6b), 4.84 (dd, 1H, J = 14.5 and 6.2 Hz, H-3'a), 4.69 (dd, 1H, J = 14.1 and 4.3 Hz, H-3'b), 5.00 (br s, 1H, H-1), 5.29 (s, 2H, CH_2), 5.30–5.34 (m, 2H, H-4 and H-2′), 5.81 (ddd, 1H, J = 10.2, 2.7 and 1.9 Hz, H-2), 5.92 (br d, 1H, *J* = 10.2 Hz, H-3), 7.07 (app dt, 2H, J = 9.0 and 1.7 Hz, H_{Ar}), 7.66 (s, 1H, H_{triaz}), 8.00 (app dt, 2H, J = 9.0 and 1.9 Hz, H_{Ar}). ^{13}C NMR (100 MHz): δ 12.3 (CH_3), 20.7 ($\underline{C}H_3CO$), 20.8 ($\underline{C}H_3CO$), 20.9 ($\underline{C}H_3CO$), 50.1 (C-1′), 62.0 (CH_2OAr), 62.8 (C-6), 65.1 (C-4), 66.3 (C-3′), 67.2 (C-5), 70.4 (C-2′), 94.6 (C-1), 115.0 ($2C_{Ar}$), 119.9 (C_{Ar}), 123.6 (C5'$_{triaz}$), 126.8 (C-2), 129.0 ($2C_{Ar}$), 129.8 (C-3), 144.0 (C4'$_{triaz}$), 160.3 (C_{Ar}), 167.9 (C_{oxad}), 169.7 (OAc), 170.2 (OAc), 170.7 (OAc), 176.3 (C_{oxad}). ESI-HRMS calcd for $C_{27}H_{32}N_5O_{10}$ $[M+H]^+$: 586.2143; found: 586.2143.

*4.1.3. 15 1′-O-(4,6-di-O-acetyl-2,3-dideoxy-α-D-erythro-hex-2- enopiranosyl)-(2′-acetyl-3′-deoxy-[4-(n-decil)]-1,2,3-triazol-1-yl-sn-glycerol (**9**).* Yield 87%, colorless oil, $[\alpha]_D^{25}$ = + 34 (*c* 0.1, CH_2Cl_2), R_f 0.53 (Hexano/EtOAcO, 1:1). ^{1}H NMR (400 MHz): δ 0.88 (t, 3H, *J* = 7.1 Hz, CH_3), 1.26–1.32 (m, 12H, 6 CH_2), 1.64–1.67 (m, 4H, 2 x CH_2), 2.07 (s, 3H, CH_3), 2.09 (s, 3H, CH_3), 2.10 (s, 3H, CH_3), 2.71 (t, 2H, *J* = 7.8 Hz, CH_2), 3.58 (dd, 1H, J = 10.6 and 4.7 Hz, H-1'a), 3.86 (dd, 1H, J = 10.6 and 5.1 Hz, H-1'b), 4.10 (ddd, 1H, J = 9.8, 4.7 and 2.4 Hz, H-5), 4.18 (dd, 1H, J = 12.1 and 2.7 Hz, H-6a), 4.27 (dd, 1H, J = 12.2 and 5.1 Hz, H-6b), 4.57 (dd, 1H, J = 14.4 and 6.3 Hz, H-3'a), 4.64 (dd, 1H, J = 14.5 and 4.7 Hz, H-3'b), 5.02 (br s, 1H, H-1), 5.29–5.33 (m, 2H, H-2′ and H-4), 5.83 (ddd, 1H, J = 10.2, 2.6 and 2.0 Hz, H-2), 5.93 (br d, 1H, *J* = 10.2 Hz, H-3), 7.30 (s, 1H, H_{triaz}). ^{13}C NMR (100 MHz): δ 14.1 (CH_3), 20.7 ($\underline{C}H_3CO$), 20.8 ($\underline{C}H_3CO$), 20.9 ($\underline{C}H_3CO$), 22.6 (CH_2), 25.6 (CH_2), 29.2 (CH_2), 29.3 (CH_2), 29.4 (CH_2), 29.4 (CH_2), 29.5 (CH_2), 29.6 (CH_2), 31.9 (CH_2-triaz), 49.8 (C-1′), 62.8 (C-6), 65.1 (C-4), 66.5 (C-3′), 67.2 (C-5), 70.7 (C-2′), 94.7 (C-1), 121.3 (C5'$_{triaz}$), 127.0 (C-2), 129.8 (C-3), 148.7 (C4'$_{triaz}$), 169.8 (OAc), 170.2 (OAc), 170.7 (OAc). ESI-HRMS calcd for $C_{27}H_{43}N_3O_8$ $[M+H]^+$: 538.3123; found: 538.3124.

*4.1.4. Synthesis of bis-1H-1,2,3-triazole/1,2,4-oxadiazoles **(10 and 11)***

$CuSO_4 \cdot 5H_2O$ (0.12 mmol), sodium ascorbate (0.18 mmol) and bis-alkyne (**3l** or **3m**) (0.2 mmol) were mixed in water (1.5 mL) in a Schlenk flask under argon. This mixture was added into another Schlenk flask containing 0.5 mmol of the azido-carbohydrate **4** dissolved in 2 mL of dichloromethane. The mixture was stirred at room temperature for 45 min. Then, the solvent was removed, and the residue was purified by column chromatography using ethyl acetate.

*4.1.4.1. N-Cyclohexyl-N-[4,4'-[(1,4-phenylene)-bis(1′-O-(4,6-di-O-acetyl-2,3-dideoxy-α-D-erythro-hex-2-enopyranosyl)-(2′-acetyl-3′-deoxy)-di-(1H-1,2,3-triazol-1-yl)]methyl-sn-glyceryl-1,2,4-oxadiazol-5-amine (**10**).* Yield 62% (130 mg), colorless oil, $[\alpha]_D^{25}$ = + 20 (*c* 0.1, CH_2Cl_2); R_f 0.6 (EtOAc). ^{1}H NMR (300 MHz): δ 1.16–1.43, 1.55–1.88 (m, 10H, cyclohexyl), 1.96 (s, 3H, CH_3), 2.07–2.11 (s, 15H, 5xCH_3), 3.54 (dd, 1H, J = 10.6 and 4.1 Hz, H-3'a1), 3.64 (dd, 1H, J = 10.6 and 4.5 Hz, H-3'a2), 3.83 (dd, 1H, J = 10.6 and 5.3 Hz, H-3'b1), 3.89 (dd, 1H, J = 10.5 and 5.3 Hz, H-3'b2), 3.98–4.03 (m, 1H, N–CH), 4.08 (ddd, 1H, J = 10.0, 5.3 and 2.3 Hz, H-5a), 4.13 (ddd, 1H, J = 9.4, 4.1 and 2.3 Hz, H-5b), 4.16–4.17 (m, 1H, H-6a), 4.23–4.30 (m, 3H, H-6a′, H-6b and H-6b′), 4.58 (dd, 1H, J = 14.1 and 6.5 Hz, H-1'a1), 4.64 (dd, 1H, J = 14.1 and 4.7, H-1'a2), 4.71–4.74 (m, 2H, H-1'b1 and H-1'b2), 4.78 (br s, 2H, CH_2–N), 4.98 (br s, 1H, H-1a), 5.05 (br s, 1H, H-1b),

5.26–5.42 (m, 4H, H-4a, H-4b, H-2′ and H-2''), 5.78 (app dt, 1H, J = 10.6, 1.7 and 1.7 Hz, H-2a), 5.85 (app dt, 1H, J = 10.5, 2.3 and 2.3 Hz, H-2b), 5.89 (d, 1H, *J* = 10.7 Hz, H-3), 5.95 (d, 1H, *J* = 10.5 Hz, H-3), 7.71 (s, 1H, H-5'$_{triaz}$), 7.90 (s, 1H, H-5''$_{triaz}$), 7.92 (d, 2H, *J* = 8.8 Hz, H_{Ar}), 8.09 (d, 2H, *J* = 8.8 Hz, H_{Ar}). ^{13}C NMR (75 MHz): δ 20.6 ($\underline{C}H_3CO$), 20.7 (2 x $\underline{C}H_3CO$), 20.8 ($\underline{C}H_3CO$), 20.9 (2 x $\underline{C}H_3CO$), 25.1 (C-cyclohexyl), 25.7 (2C-cyclohexyl), 30.8 (2C, cyclohexyl), 40.4 (N-$C_{cyclohexyl}$), 50.0 and 50.1 (2 x C-1′), 59.4 (CH_2N-$C_{cyclohexyl}$), 62.8 (2 x C-6), 65.0 and 65.1 (2 x C-4), 66.3 (2 x C-3′), 67.1 and 67.2 (2 x C-5), 70.4 and 70.5 (2 x C-2′), 94.6 and 94.7 (2 x C-1), 120.9 (C5'$_{triaz}$), 124.1 (C5'$_{triaz}$), 125.8 (2C_{Ar}), 126.8 and 126.9 (2 x C-2), 127.6 (C_{Ar}), 127.7 (2C_{Ar}), 129.7 and 129.8 (2 x C-3), 132.6 (C_{Ar}), 145.0 and 147.3 (2 x C4'$_{triaz}$), 168.0 (C_{oxad}), 169.6 (C_{oxad}), 169.9 (OAc), 170.2 (2 x OAc), 170.6 (OAc), 170.7 (OAc), 171.1 (OAc). ESI-HRMS calcd for $C_{49}H_{62}N_9O_{17}$ $[M+H]^+$: 1048.4264; found: 1048.4268.

*4.1.4.2. N-Cyclohexyl-N-[4,4'-[(1,4-phenylene)-bis(1′-O-(4,6-di-O-acetyl-2,3-dideoxy-α-D-erythro-hex-2-enopyranosyl)-(2′-acetyl-3′-deoxy)-di-(1H-1,2,3-triazol-1-yl)]methoxyphenyl-sn-glyceryl-1,2,4-oxadiazol-5-amine (**11**).* Yield 67% (144,5 mg), colorless oil, $[\alpha]_D^{25}$ = + 35 (*c* 0.2, CH_2Cl_2); R_f 0.5 (EtOAc). ^{1}H NMR (300 MHz): δ 1.15–1.43, 166–1.86 (m, 10H, cyclohexyl), 1.95 (s, 3H, CH_3), 2.03 (s, 3H, CH_3), 2.07 (s, 3H, CH_3), 2.08 (s, 3H, CH_3), 2.08 (s, 3H, CH_3), 2.09 (s, 3H, CH_3), 3.53 (dd, 1H, *J* = 10.6 and 4.7 Hz, H-3'a1), 3.59 (dd, 1H, *J* = 10.6 and 4.7 Hz, H-3'a2), 3.82 (dd, 1H, *J* = 5.2 and 2.3 Hz, H-3'b1), 3.85 (dd, 1H, *J* = 5.9 and 1.8 Hz, H-3'b2), 3.95–4.02 (m, 1H, N–CH, cyclohexyl), 4.05–4.30 (m, 6H, H-5a, H-5b, H-6a, H-6a′, H-6b and H6b′), 4.54–462 (m, 2H, H-1'a1 and H-1'a2), 4.65–4.71 (m, 2H, H-1'b1 and H-1'b2), 4.76 (s, 2H, N–CH_2), 4.98 (br s, 1H, H-1a), 5.01 (br s, 1H, H-1b), 5.27 (br s, 2H, CH_2O), 5.31–5.33 (m, 4H, H-4a, H-4b, H-2′ and H-2''), 5.76–5.83 (m, 2H, H-2a and H-2b), 5.87–5.95 (m, 2H, H-3◦ and H-3b), 7.03 (d, 2H, *J* = 8.8 Hz, H_{Ar}), 7.68 (s, 1H, H_{triaz}), 7.69 (s, 1H, H_{triaz}), 7.94 (d, 2H, *J* = 8.8 Hz, H_{Ar}). ^{13}C NMR (75 MHz): δ 20.6 ($\underline{C}H_3CO$), 20.7 (2 x $\underline{C}H_3CO$), 20.8 ($\underline{C}H_3CO$), 20.9 (2 x $\underline{C}H_3CO$), 25.1 (C-cyclohexyl), 25.7 (2C-cyclohexyl), 30.8 (2C, cyclohexyl), 40.4 (N-$C_{cyclohexyl}$), 50.0 and 50.1 (2 x C-1′), 59.3 (CH_2N-$C_{cyclohexyl}$), 62.0 (CH_2OAr), 62.8 (2 x C-6), 65.1 (2 x C-4), 66.3 (2 x C-3′), 67.1 and 67.2 (2 x C-5), 70.4 (2 x C-2′), 94.5 and 94.6 (2 x C-1), 114.8 (2C_{Ar}), 120.9 (C5'$_{triaz}$), 123.6 (C_{Ar}), 124.0 (C5'$_{triaz}$), 126.8 (2 x C-2), 128.8 (2C_{Ar}), 129.7 and 129.8 (2 x C-3), 145.1 (C_{Ar}), 160.1 (2 x C4'$_{triaz}$), 168.0 (C_{oxad}), 169.6 (C_{oxad}), 169.7 (OAc), 170.2 (2 x OAc), 170.7 (2 x OAc), 171.0 (OAc). ESI-HRMS calcd for $C_{50}H_{64}N_9O_{18}$ $[M+H]^+$: 1078.4369; found: 1078.4364.

4.2. Biological evaluation

4.2.1. Cytotoxicity studies

Cells: Human tumor cell lines PC-3 (prostate adenocarcinoma), HCT-116 (colorectal tumor), NCIH 460 (lung carcinoma), SKMEL-103 (melanoma) and AGP-01 (gastric tumor) were used. The cells were ceded by the National Cancer Institute (USA) and grown in RPMI 1640 medium (PC-3, HCT-116, and NCIH-460) and in Dulbecco's Modified Eagle Medium (DMEM) (SKMEL-103 and AGP-01), both supplemented with 10% of bovine fetal serum and 1% of antibiotics, kept in the incubator at 37 °C and atmosphere containing 5% of CO_2.

Compounds: All samples were diluted in sterile pure DMSO at the stock concentration of 10 mM/1 mL, following laboratory standard conditions.

Method: MTT cytotoxicity analysis is one of the methods used in the United States National Cancer Institute (NCI) screening program, which tests more than 10,000 samples each year [55]. It is a fast, sensitive, and inexpensive method, first described by Mossman (1983). This method is able to analyze the viability and metabolic state of the cell. It is a colorimetric analysis based on the conversion of tetrazolium 3-(4,5-dimethyl-2-thiazol)-2,5-diphenyl-2-H-bromide (MTT) salt to formazan from mitochondrial enzymes present only in metabolically active cells [56]. The cytotoxic study by the MTT method allows to easily define the cytotoxicity, but not the mechanism of action [57]. Tumor cells were previously maintained in 75 cm^2 cell culture flasks and further seeded in 96-well plates at concentrations 0.3 x 10^6 cells/mL for SKMEL-103 and AGP-01; 0.1x10^6 cells/mL for PC-3 and NCIH-460 and 0.7 x 10^5 cells/mL for the HCT-116. The cells were incubated with the compounds at a single concentration of 25 μM for 72 h in a 5% CO_2 incubator at 37 °C. At the end of this, they were centrifuged (400×*g* for 5 min) and the supernatant was removed. Then 100 μL of 1% MTT (tetrazolium salt) solution was added, and the plates were incubated for 3 h. The absorbance was read after dissolution of the precipitate in 150 μL of pure DMSO in a 570 nm plate spectrophotometer.

Statistical analysis: The absorbances obtained were used to calculate the IC50 values by nonlinear regression employing appropriate statistical software. Statistical significance was calculated by Analysis of Variance (ANOVA) followed by Tukey's test, with a significance level of $p < 0.05$.

Cytotoxicity using Vero cells: Vero cells were grown in Dulbecco's modified Eagle's medium (DMEM) (Gibco, Carlsbad, CA) supplemented with 10% inactivated fetal bovine serum (FBS) (Gibco), 2 mM L-glutamine (Gibco) and 100 U/mL penicillin/streptomycin (Gibco). The toxicity of the synthesized compounds was evaluated on growing cells using the MTT method (Sigma, St. Louis, USA) as previously described [58]. Briefly, Vero cells (1 × 10^4 cells/well) were plated in 96-well microplates 24 h in advance and thentreated with various concentrations of the compounds (800, 400, 200, 100, 50 μM) in max. 0.8% of DMSO. After 5 days of incubation at 37 °C, culture medium was removed and was replenished with 50 μL of MTT solution (1 mg/mL) per well and the microplate was incubated for additional 4 h. MTT formazan crystals were solubilised by adding dimethylsulfoxide (DMSO) and the optical density at 570 nm (OD570) was determined by spectrophotometry using a BioTekTM ELx800TM 96 well plate reader (BioTekInstrumentsInc.,Winooski,VT). Cell viability was calculated by subtracting the OD at 570 nm of treated cells from untreated control cells. The cytotoxic concentration for 50% of the cell culture (CC50) was defined as the concentration of compound that caused a 50% reduction in absorbance.

4.2.2. In vitro antitubercular activity evaluation

Reference Strain: Mycobacterium tuberculosis H37Ra (ATCC 25177) and H37Rv (ATCC 27294) from American Type Culture Collection (Manassas, VA) were used.

Commercial drugs and chemicals: Rifampicin (RIF), ethambutol (EMB) (Sigma-Aldrich NV/SA, Bornem, Belgium) solutions were prepared at concentrations of 1 mg/mL in distilled water and 10 mg/mL in methanol, respectively, filter sterilized and frozen until used.

Determination of Minimum Inhibitory Concentration (MIC): The *in vitro* assay for the determination of minimum inhibitory concentration (MIC) was performed in duplicate by Resazurin Microtiter Assay Plate (REMA) as described previously by Palomino et al. [59] with modifications. RIF and EMB solutions were thawed and diluted in 7H9–S medium. Serial two-fold dilutions of each drug in 100 μL of 7H9–S medium were prepared directly in 96-well plates at concentrations of 2.0 to 0.0625 μg/mL for RIF and 16.0 to 0.5 μg/mL for EMB. Serial two-fold dilutions of the triazole derivatives solutions were performed directly on the microplate, with a concentration ranging from 64 μg/mL to 0.5 μg/mL. Growth controls containing no antibiotic and sterility controls without inoculation were also included. The inoculum used was prepared from fresh

Löwenstein Jensen medium in 7H9—S medium adjusted to a McFarland tube no. 1 and then diluted 1:20 and 100 μL. The plates were covered, sealed in plastic bags, and incubated at 37 °C under normal atmosphere. After 9 days of incubation, 30 μL of resazurin solution was added to each well, incubated overnight at 37 °C, and assessed for color development. Resazurin sodium salt powder (Acros Organic N·V., Geel, Belgium) was prepared at 0.01% (wt/vol) in distilled water and filter sterilized. A change from blue to pink indicates reduction of resazurin and therefore bacterial growth. The MIC was defined as the lowest drug concentration that prevented this color change. The cut-off points for susceptibility/resistance to antimicobacterial strains were 0.5 and 5 μg/mL for RIF and EMB, respectively [60].

Cytotoxicity test: Raw 264.7 (ATCC TIB - 71) macrophages e HepG2 cells were used to assess cell cytotoxicity by MTT [3-(4,5-dimethylthiazol-2-yl)-2,5-diphenyl-2H-tetrazolium bromide, Sigma, USA]. The cell line was cultured in DMEM medium, at 37 °C in a humidified atmosphere of 5% CO2. The culture medium was changed after 2—3 days and subcultured when cell population density reached to 70—80% confluence. Macrofages 10^5 cells/well were added in 96-well plates and incubated for 24 h (37 °C and 5% CO_2). Compounds were then added in different concentrations (1—100 mg/mL) and incubated for 48 h. Untreated, rifampicin (RIF), ethambutol (EMB) were employed as controls. Experiments were performed in duplicate. MTT (3-(4,5-dimethylthiazol-2-yl)-2,5-diphenyl-2H-tetrazolium bromide, 5 mg/mL in PBS) was added to each well and incubated again for 2 h. Culture medium and non reduced MTT were removed and 100 μL of DMSO were added. The amount of formazan was determined by measuring the absorbance at 570 nm. The negative control was obtained in wells containing only culture medium and cells (without treatment). Cytotoxic concentration for 50% inhibition of viability (CC_{50}) was also calculated by regression analysis using GraphPad Prism software. The selectivity index (SI) was determined as the ratio of CC_{50} values (cell lines) and inhibitory concentration for 50% bacterial, MIC (SI = IC_{50}/MIC); since SI $\geq$ 10 or greater indicates when the test compound can be applied at concentration ten times or more above the MIC value without presenting cytotoxicity [42,43].

4.3. Molecular docking study

4.3.1. Homology modelling and structure validation

The crystal structure of DprE1 and InhA proteins were downloaded from RCSB database (www.rcsb.org). The stereo-chemical geometry of residues was measured by Ramachandran map (By Procheck) [61]. The computational work was performed using Schrodinger software (Schrodinger release 2020-1 license dated November 20, 2020).

4.3.2. Preparation of protease structure and active site identification

The structure of both proteins was prepared prior docking to resolve several structural issues such as missing hydrogen atoms, incorrect bond order, ionization states using Epik, missing loop in protein as well as missing side chains of residues [62,63]. Strained bonds/angles as well as steric clashes were also rectified through restrained energy minimization during protein preparation which allowed movement in heavy atoms up to 0.3 Å. The forcefield OPLS2005 [64] was used for this in-silico study.

4.3.3. Ligand preparation

The compound **5e** and **7** was prepared by Ligprep tool prior to docking [65]. The ionization state was determined for ligands using Epik at pH 7 ± 2 as well as tautomers were generated [66].

4.3.4. Molecular docking of designed chemical library

Site specific molecular flexible docking was performed on glide platform against DprE1 and InhA protein of *Mycobacterium tuberculosis* [67]. These molecules were docked at extra precision and analyzed for docking score. The ΔGº were also calculated by using prime mmgbsa for both compounds [63].

4.3.5. Molecular dynamics (MD) simulation

Molecular dynamic simulation was done to validate docking observations for both molecules in complex with both proteins. The simulation was done for 100ns time period on Desmond software to visualize the binding and conformational stability of both molecules with in binding pocket [68]. The complex was solvated TIP3P water model prior to simulation where 0.15 M NaCl added to mimic a physiological ionic concentration.

Declaration of competing interest

The authors declare that they have no known competing financial interests or personal relationships that could have appeared to influence the work reported in this paper.

Acknowledgment

The authors are grateful to National Council for Scientific and Technological Development - CNPq [grant numbers 448082/2014-4, PQ 301308/2017-9] and LABEX SYNORG [grant number ANR-11-LABX-0029] for financial support. This study was financed in part by the Coordenação de Aperfeiçoamento de Pessoal de Nível Superior — Brasil - CAPES finance code 001. We are indebted with Daniele Mendes Felix by the cytotoxicity evaluated in Vero cell for four compounds. Our thanks are also extended to Analytical Centers CENAPESQ-UFRPE and DQF-UFPE. BR and PPS acknowledge the administration of Hansraj College, University of Delhi for infrastructural support.

Appendix A. Supplementary data

Supplementary data to this article can be found online at https://doi.org/10.1016/j.ejmech.2021.113472.

References

[1] D.P. Galonić, D.Y. Gin, Chemical glycosylation in the synthesis of glycoconjugate antitumour vaccines, Nature 446 (2007) 1000—1007, https://doi.org/10.1038/nature05813.
[2] S. Dedola, S.A. Nepogodiev, R.A. Field, Recent applications of the Cu^I-catalysed Huisgen azide—alkyne 1,3-dipolar cycloaddition reaction in carbohydrate chemistry, Org. Biomol. Chem. 5 (2007) 1006—1017, https://doi.org/10.1039/B618048P.
[3] S. Chittaboina, F. Xie, Q. Wang, One-pot synthesis of triazole-linked glycoconjugates, Tetrahedron Lett. 46 (2005) 2331—2336, https://doi.org/10.1016/j.tetlet.2005.01.175.
[4] M.J. Sofia, Generation of oligosaccharide and glycoconjugate libraries for drug discovery, Drug Discov. Today 1 (1996) 27—34, https://doi.org/10.1016/1359-6446(96)89116-1.
[5] World Health Organization, Target Product Profiles for Tuberculosis Preventive Treatment, 2020 accessed august 28.
[6] World Health Organization - Global Tuberculosis Report. https://www.who.int/tb/publications/global_report/en/, 2019. (Accessed 28 August 2020).
[7] S. Motamen, R.J. Quinn, Analysis of approaches to anti-tuberculosis compounds, ACS Omega 5 (2020) 28529—28540, https://doi.org/10.1021/acsomega.0c03177.
[8] M.M. Abdel-Aziz, M.H. Abu Elella, R.R. Mohamed, Green synthesis of quaternized chitosan/silver nanocomposites for targeting mycobacterium tuberculosis and lung carcinoma cells (A-549), Int. J. Biol. Macromol. 142 (2020) 244—253, https://doi.org/10.1016/j.ijbiomac.2019.09.096.
[9] World Health Organization. https://www.who.int/news-room/fact-sheets/detail/cancer. (Accessed 28 August 2020).
[10] M.B.R. Oliveira, L.C. Souza, E.J.G. Sampayo, G.S. Carvalho, F.C.Q. Mello, M.E.M. Paschoal, The impact of lung carcinoma histology on the frequency of

bone metastases, Rev. Bras. Ortop. 54 (2019) 524–530, https://doi.org/10.1016/j.rbo.2018.02.002.
[11] M. Chai, Q. Shi, The effect of anti-cancer and antituberculosis treatments in lung cancer patients with active tuberculosis: a retrospective analysis, BMC Canc. 20 (2020) 1121, https://doi.org/10.1186/s12885-020-07622-6.
[12] N. Alsaad, B. Wilffert, R. van Altena, W.C.M. de Lange, T.S. van der Werf, J.G.W. Kosterink, J.-W.C. Alffenaar, Potential antimicrobial agents for the treatment of multidrug-resistant tuberculosis, Eur. Respir. J. 43 (2014) 884–897, https://doi.org/10.1183/09031936.00113713.
[13] B. Bhukya, A. Shukla, V. Chaturvedi, P. Trivedi, S. Kumar, F. Khan, A.S. Negi, S.K. Srivastava, Design, synthesis, *in vitro* and *in silico* studies of 2,3-diaryl benzofuran derivatives as antitubercular agents, Bioorg. Chem. 99 (2020), 103784, https://doi.org/10.1016/j.bioorg.2020.103784.
[14] F.J. Smit, R. Seldon, J. Aucamp, A. Jordaan, D.F. Warner, D.D. N'Da, Synthesis and antimycobacterial activity of disubstituted benzyltriazoles, Med. Chem. Res. 28 (2019) 2279–2293, https://doi.org/10.1007/s00044-019-02458-7.
[15] S. Pathania Archna, P.A. Chawla, Thiophene-based derivatives as anticancer agents: an overview on decade's work, Bioorg. Chem. 101 (2020) 104026, https://doi.org/10.1016/j.bioorg.2020.104026.
[16] S.D. Joshi, S.R. Dixit, M.N. Kirankumar, T.M. Aminabhavi, K.V.S.N. Raju, R. Narayan, C. Lherbet, K.S. Yang, Synthesis, antimycobacterial screening and ligand-based molecular docking studies on novel pyrrole derivatives bearing pyrazoline, isoxazole and phenyl thiourea moieties, Eur. J. Med. Chem. 107 (2016) 133–152, https://doi.org/10.1016/j.ejmech.2015.10.047.
[17] K. Pyta, K. Klich, J. Domagalska, P. Przybylski, Structure and evaluation of antibacterial and antitubercular properties of new basic and heterocyclic 3-formylrifamycin SV derivatives obtained via 'click chemistry' approach, Eur. J. Med. Chem. 84 (2014) 651–676, https://doi.org/10.1016/j.ejmech.2014.07.066.
[18] C.S. Santos, R.J. de Oliveira, R.N. de Oliveira, J.C.R. Freitas, 1,2,3- Triazoles: general and key synthetic strategies, Arkivoc, part i (2020) 219–271, https://doi.org/10.24820/ark.5550190.p011.293.
[19] V.N.M. de Oliveira, F.G. dos Santos, V.P.G. Ferreira, H.M. Araújo, C. Ó Pessoa, R. Nicolete, R.N. de Oliveira, Focused microwave irradiation-assisted synthesis of N-cyclohexyl-1,2,4-oxadiazole derivatives with antitumor activity, Synth. Commun. 48 (2018) 2522–2532, https://doi.org/10.1080/00397911.2018.1509350.
[20] S.K. Verma, R. Verma, S. Verma, Y. Vaishnav, S.P. Tiwari, K. P Rakesh, Anti-tuberculosis activity and its structure-activity relationship (SAR) studies of oxadiazole derivatives: a key review, Eur. J. Med. Chem. 209 (2021), 112886, https://doi.org/10.1016/j.ejmech.2020.112886.
[21] S. Zhang, Z. Xu, C. Gao, Q.-C. Ren, L. Chang, Z.-S. Lv, L.-S. Feng, Triazole derivatives and their anti-tubercular activity, Eur. J. Med. Chem. 138 (2017) 501–513, https://doi.org/10.1016/j.ejmech.2017.06.051.
[22] N.D. Thanh, D.S. Hai, N.T.T. Ha, D.T. Tung, C.T. Le, H.T.K. Van, V.N. Toan, D.N. Toan, L.H. Dang, Synthesis, biological evaluation and molecular docking study of 1,2,3-1H-triazoles having 4H-pyrano[2,3-d]pyrimidine as potential Mycobacterium tuberculosis protein tyrosine phosphatase B inhibitors, Bioorg. Med. Chem. Lett 29 (2019) 164–171, https://doi.org/10.1016/j.bmcl.2018.12.009.
[23] P.S. Phatak, R.D. Bakale, R.S. Kulkarni, S.T. Dhumal, P.P. Dixit, V.S. Krishna, D. Sriram, V.M. Khedkar, K.P. Haval, Design and synthesis of new indanol-1,2,3-triazole derivatives as potent antitubercular and antimicrobial agents, Bioorg. Med. Chem. Lett 30 (2020), 127579, https://doi.org/10.1016/j.bmcl.2020.127579.
[24] M. Muthukrishnan, M. Mujahid, P. Yogeeswari, D. Sriram, Syntheses and biological evaluation of new triazole-spirochromone conjugates as inhibitors of Mycobacterium tuberculosis, Tetrahedron Lett. 52 (2011) 2387–2389, https://doi.org/10.1016/j.tetlet.2011.02.099.
[25] K.M. Naidu, S. Srinivasarao, N. Agnieszka, A.K. Ewa, M.M.K. Kumar, K.V.G.C. Sekhar, Seeking potent anti-tubercular agents: design, synthesis, anti-tubercular activity and docking study of various ((triazoles/indole)-piperazin-1-yl/1,4-diazepan-1-yl)benzo[d]isoxazole derivatives, Bioorg. Med. Chem. Lett 26 (2016) 2245–2250, https://doi.org/10.1016/j.bmcl.2016.03.059.
[26] T.G. Shruthi, S. Eswaran, P. Shivarudraiah, S. Narayanan, S. Subramanian, Synthesis, antituberculosis studies and biological evaluation of new quinoline derivatives carrying 1,2,4-oxadiazole moiety, Bioorg. Med. Chem. Lett 29 (2019) 97–102, https://doi.org/10.1016/j.bmcl.2018.11.002.
[27] F. Gao, Z. Chen, L. Ma, Y. Fan, L. Chen, G. Lu, Synthesis and biological evaluation of moxifloxacin-acetyl-1,2,3-1H-triazole-methylene-isatin hybrids as potential anti-tubercular agents against both drug-susceptible and drug-resistant Mycobacterium tuberculosis strains, Eur. J. Med. Chem. 180 (2019) 648–655, https://doi.org/10.1016/j.ejmech.2019.07.057.
[28] S. Mishra, K. Upadhaya, K.B. Mishra, A.K. Shukla, R.P. Tripathi, V.K. Tiwari, Chapter 10 - carbohydrate-based therapeutics: a frontier in drug discovery and development, Stud. Nat. Prod. Chem. 49 (2016) 307–361, https://doi.org/10.1016/B978-0-444-63601-0.00010-7.
[29] I. Velter, B. La Ferla, F. Nicotra, Carbohydrate-based molecular scaffolding, J. Carbohydr. Chem. 25 (2006) 97–138, https://doi.org/10.1080/07328300600733020.
[30] E. Lenci, G. Menchi, A. Trabocchi, Carbohydrates in diversity-oriented synthesis: challenges and opportunities, Org. Biomol. Chem. 14 (2016) 808–825, https://doi.org/10.1039/C5OB02253C.
[31] R.N. de Oliveira, D. Sinou, R.M. Srivastava, A Very Simple Synthesis of 1-(Ethyl 6-O-Acetyl-2,3,4-Trideoxy-α-D-Erythro-Hex-2-Enopyranos-4-Yl)-1,2,3-Triazole Derivatives, Synthesis, 2006, pp. 467–470, https://doi.org/10.1055/s-2006-926280.
[32] P.L.F. da Costa, V.N. Melo, B.M. Guimarães, M. Schuler, V. Pimenta, P. Rollin, A. Tatibouët, R.N. de Oliveira, Glycerol carbonate in Ferrier reaction: access to new enantiopure building blocks to develop glycoglycerolipid analogues, Carbohydr. Res. 436 (2016) 1–10, https://doi.org/10.1016/j.carres.2016.10.009.
[33] Shaveta, S. Mishra, P. Singh, Hybrid molecules: the privileged scaffolds for various pharmaceuticals, Eur. J. Med. Chem. 81 (2014) 301–313, https://doi.org/10.1016/j.ejmech.2014.05.005.
[34] D.F. Aguiar, L.L.A. Dutra, W.M. Dantas, G.G.C. de Carvalho, R.P.G. Lemes, C.O. Pessoa, C.R.K. Paier, P.L.B. Araujo, E.S. Araujo, L.J. Pena, R.N. de Oliveira, Synthesis, antitumor and cytotoxic activity of new adamantyl *O*-acylamidoximes and 3-aryl-5-adamantane-1,2,4-oxadiazole derivatives, Chemistry 4 (2019) 9112–9118, https://doi.org/10.1002/slct.201901285.
[35] J.V. dos Anjos, D. Sinou, S.J. de Melo, R.M. Srivastava, Synthesis of glycosyl-triazole linked 1,2,4-oxadiazoles, Carbohydr. Res. 342 (2007) 2440–2449, https://doi.org/10.1016/j.carres.2007.07.011.
[36] J.V. dos Anjos, R.A.W. Neves Filho, S.C. do Nascimento, R.M. Srivastava, S.J. de Melo, D. Sinou, Synthesis and cytotoxic profile of glycosyl–triazole linked to 1,2,4-oxadiazole moiety at C-5 through a straight-chain carbon and oxygen atoms, Eur. J. Med. Chem. 44 (2009) 3571–3576, https://doi.org/10.1016/j.ejmech.2009.03.002.
[37] Y. Naro, N. Ankenbruck, M. Thomas, Y. Tivon, C.M. Connelly, L. Gardner, A. Deiters, Small molecule inhibition of MicroRNA miR-21 rescues chemosensitivity of renal-cell carcinoma to topotecan, J. Med. Chem. 61 (2018), https://doi.org/10.1021/acs.jmedchem.7b01891, 5900–5909.
[38] V. Cukic, The association between lung carcinoma and tuberculosis, Med. Arch. 71 (2017) 212–214, https://doi.org/10.5455/medarh.2017.71.212-214.
[39] H.T. Lee, K.H. Jung, S.K. Kim, M.R. Choi, Y.G. Chai, Effects of pargyline on cellular proliferation in human breast cancer cells, Mol. Cell. Toxicol. 8 (2012) 393–399, https://doi.org/10.1007/s13273-012-0048-y.
[40] K. Lutsenko, S. Hagenow, A. Affini, D. Reiner, H. Stark, Rasagiline derivatives combined with histamine H3 receptor properties, Bioorg. Med. Chem. Lett 29 (2019), 126612, https://doi.org/10.1016/j.bmcl.2019.08.016.
[41] H.Z. Zhang, S. Kasibhatla, J. Kuemmerle, W. Kemnitzer, K. Ollis-Mason, L. Qiu, C. Crogan-Grundy, B. Tseng, J. Drewe, S.X. Cai, Discovery and Structure–Activity relationship of 3-Aryl-5-aryl-1,2,4-oxadiazoles as a new series of apoptosis inducers and potential anticancer agent, J. Med. Chem. 48 (2005) 5215–5223, https://doi.org/10.1021/jm050292k.
[42] I. Orme, Search for new drugs for treatment of tuberculosis, Antimicrob. Agents Chemother. 47 (2001) 1943–1946, https://doi.org/10.1128/AAC.45.7.1943-1946.2001.
[43] K. Katsuno, J.N. Burrows, K. Duncan, R.H. van Huijsduijnen, T. Kaneko, K. Kita, C.E. Mowbray, D. Schmatz, P. Warner, B.T. Slingsby, Hit and lead criteria in drug discovery for infectious diseases of the developing world, Nat. Rev. Drug Discov. 14 (2015) 751–758, https://doi.org/10.1038/nrd4683.
[44] M.I. Islam, H. Seo, S. Kim, V.S. Sadu, K.-I. Lee, H.-Y. Song, Antimicrobial activity of IDD-B40 against drug-resistant Mycobacterium tuberculosis, Sci. Rep. 11 (2021) 740, https://doi.org/10.1038/s41598-020-80227-y.
[45] J.S. Khara, B. Mojsoska, D. Mukherjee, P.R. Langford, B.D. Robertson, H. Jenssen, P.L. Rachel Ee, S.M. Newton, Ultra-short antimicrobial peptoids show propensity for membrane activity against multi-drug resistant Mycobacterium tuberculosis, Front. Microbiol. 11 (2020) 417, https://doi.org/10.3389/fmicb.2020.00417.
[46] J. Smith, H. Wescott, J. Early, S. Mullen, J. Guzman, J. Odingo, J. Lamarb, T. Parish, Anthranilic amide and imidazobenzothiadiazole compounds disrupt Mycobacterium tuberculosis membrane potential, MedChemComm 10 (2019) 934–945, https://doi.org/10.1039/c9md00088g.
[47] M. Bokhari, R.J. Carnachan, N.R. Cameron, S.A. Przyborski, Culture of HepG2 liver cells on three dimensional polystyrene scaffolds enhances cell structure and function during toxicological challenge, J. Anat. 211 (2007) 567–576, https://doi.org/10.1111/j.1469-7580.2007.00778.x.
[48] L. Merly, S.L. Smith, Murine RAW 264.7 cell line as an immune target: are we missing something? Immunopharmacol. Immunotoxicol. 39 (2017) 55–58, https://doi.org/10.1080/08923973.2017.1282511.
[49] G. Riccardi, I.G. Old, S. Ekins, Raising awareness of the importance of funding for tuberculosis small-molecule research, Drug Discov, Today Off. 22 (2017) 487–491, https://doi.org/10.1016/j.drudis.2016.09.012.
[50] G. Karabanovich, J. Dusek, K. Savkova, Development of 3,5-dinitrophenyl-containing 1,2,4-triazoles and their trifluoromethyl analogues as highly efficient antitubercular agents inhibiting decaprenylphosphoryl-β- d -ribofuranose 2′-oxidase, J. Med. Chem. 62 (2019) 8115–8139, https://doi.org/10.1021/acs.jmedchem.9b00912.
[51] M.H. Shaikh, D.D. Subhedar, L. Nawale, D. Sarkar, F.A.K. Khan, J.N. Sangshetti, B.B. Shingate, 1,2,3-Triazole derivatives as antitubercular agents: synthesis, biological evaluation and molecular docking study, Med. Chem. Comm. 6 (2015) 1104–1116, https://doi.org/10.1039/C5MD00057B.
[52] T.R. Deshmukh, S.P. Khare, V.S. Krishna, D. Sriram, J.N. Sangshetti, V.M. Khedkar, B.B. Shingate, Synthesis, bioevaluation and molecular docking study of new piperazine and amide linked dimeric 1,2,3-triazoles, Synth. Commun. 50 (2020) 271–288, https://doi.org/10.1080/00397911.2019.1695275.
[53] A.A. Upare, P.K. Gadekar, H. Sivaramakrishnan, N. Naik, V.M. Khedkar, D. Sarkar, A. Choudhari, S.M. Roopan, Design, synthesis and biological

evaluation of (E)-5-styryl-1,2,4-oxadiazoles as anti-tubercular agents, Bioorg. Chem. 86 (2019) 507–512, https://doi.org/10.1016/j.bioorg.2019.01.054.
[54] C.J.P. Barros, J.J.R. de Freitas, R.N. de Oliveira, J.R. de Freitas Filho, Synthesis of amidoximes using an efficient and rapid ultrasound method, J. Chil. Chem. Soc. 56 (2011) 721–722, https://doi.org/10.4067/S0717-97072011000200022.
[55] P. Skehan, R. Storeng, D. Scudiero, A. Monks, J. McMahon, D. Vistica, J.T. Warren, H. Bodesch, S. Kenny, M.R. Boyd, New colorimetric cytotoxicity assay for anticancer – drug screening, J. Natl. Cancer Inst. 82 (1990) 1107–1112, https://doi.org/10.1093/jnci/82.13.1107.
[56] T. Mosmann, Rapid colorimetric assay for cellular growth and survival: application to proliferation and cytotoxicity assays, J. Immunol. Methods 65 (1983) 55–63, https://doi.org/10.1016/0022-1759(83)90303-4.
[57] M.V. Berridge, A.S. Tan, K.D. McCoy, R. Wang, The biochemical and cellular basis of cell proliferation assays that use tetrazolium salts, Biochemica 4 (1996) 14–19.
[58] O. V de Carvalho, D.M. Félix, L.R. de Mendonça, C.M.R.S. de Araújo, R.F.O. Franca, M.T. Cordeiro, A. Silva Jr., L.J. Pena, The thiopurine nucleoside analogue 6-methylmercaptopurine riboside (6MMPr) effectively blocks zika virus replication, Int. J. Antimicrob. Agents 50 (2017) 718–725, https://doi.org/10.1016/j.ijantimicag.2017.08.016.
[59] J.-C. Palomino, A. Martin, M. Camacho, H. Guerra, J. Swings, F. Portaels, Resazurin microtiter Assay Plate: simple and inexpensive method for detection of drug resistance in Mycobacterium tuberculosis, Antimicrob. Agents Chemother. 46 (2002) 2720–2722, https://doi.org/10.1128/AAC.46.8.2720-2722.2002.
[60] K.O. Sanchotene, A. von Groll, D. Ramos, A.B. Scholante, G. Honscha, M. Valença, C.J. Scaini, P.E.A. da Silva, Comparative evaluation of the Nitrate Reductase Assay and the Resazurin Microtitre Assay for drug susceptibility testing of Mycobacterium tuberculosis against first line anti-tuberculosis drugs, Braz. J. Microbiol. 39 (2008) 16–20, https://doi.org/10.1590/S1517-83822008000100004.
[61] R.A. Laskowski, M.W. MacArthur, D.S. Moss, J.M. Thornton, PROCHECK: a program to check the stereochemical quality of protein structures, J. Appl. Crystallogr. 26 (1993) 283–291, https://doi.org/10.1107/S0021889892009944.
[62] Schrödinger Release 2020-1: Protein Preparation Wizard; Epik, S., LLC, New York, NY, 2016; Impact, Schrödinger, LLC, New York, NY, 2016; Prime, Schrödinger, LLC, New York, NY, 2020.
[63] Schrödinger Release 2020-1: Prime, S., LLC, New York, NY, 2020.
[64] W.L. Jorgensen, J. Tirado-Rives, The OPLS [optimized potentials for liquid simulations] potential functions for proteins, energy minimizations for crystals of cyclic peptides and crambin, J. Am. Chem. Soc. 110 (1988) 1657–1666, https://doi.org/10.1021/ja00214a001.
[65] Schrödinger Release 2020-1, LigPrep, S., LLC, New York, NY, 2020.
[66] Schrödinger Release 2020-1, Epik, S., LLC, New York, NY, 2020.
[67] Schrödinger Release 2020-1, Glide, S., LLC, New York, NY, 2020.
[68] Schrödinger Release 2020-1, Desmond Molecular Dynamics System, D.E.S.R., New York, NY, Maestro-Desmond Interoperability Tools, Schrödinger, New York, NY, 2020, p. 2020.